DEVELOPMENT AND CHARACTERIZATION OF CERAMIC FOAM TILE FOR ADVANCED THERMAL PROTECTION SYSTEM

By

Sabaina Ubaid

Muhammad Ali Hamza

Muhammad Ali Mukhtar

School of Chemical and Materials Engineering

National University of Sciences and Technology

2022

DEVELOPMENT AND CHARACTERIZATION OF CERAMIC FOAM TILES FOR ADVANCED THERMAL PROTECTION SYSTEM

By

(Leader – 258237 Sabaina Ubaid)

(Member 1 – 255157 Muhammad Ali Hamza)

(Member 2 – 243779 Muhammad Ali Mukhtar)

A THESIS

Submitted to

National University of Sciences and Technology

In partial fulfillments of the requirements

For the degree of

METALLURGICAL AND MATERIAL ENGINEERING

School of Chemical and Materials Engineering (SCME)

National University of Sciences and Technology (NUST)

June, 2022

CERTIFICATE

This is to certify that work in this thesis has been completed by Ms. Sabaina ubaid, Mr. Muhammad Ali Hamza and Mr. Muhammad Ali Mukhtar under the supervision of Dr. Adeel Umar at the school of Chemical and Materials Engineering (SCME), National University of Science and Technology, H-12, Islamabad, Pakistan.

Advisor:

Dr. Adeel umar
Department of Materials Engineering
School of Chemical and Materials Engineering
National University of Sciences and Technology

Co-Advisor (if any)

Dr. ----------
Department of Materials Engineering
School of Chemical and Materials Engineering
National University of Sciences and Technology

Submitted Through:

HOD----------
Department of Materials Engineering
School of Chemical and Materials Engineering
National University of Sciences and Technology

Principal/Dean ----------
School of Chemical and Materials Engineering
National University of Sciences and Technology

DEDICATION

Dedicated to our beloved parents, family, friends and respectful teachers whose support and encouragement led us to this accomplishment.

ACKNOWLEDGEMENTS

We would like to thank Allah Almighty for giving us this opportunity and for providing us with guidance, strength and skills. Also showering his blessings upon us which enabled us to achieve this success.

We are also extremely grateful to Dr. Adeel Umer for his relentless support, and supervision during the project. It was because of his constant encouragement and mentoring that we were able to complete this project. Also would like to thank all the faculty members who assisted us throughout the project.

We would also like to thank Engr. Muhammad Zafar, Engr. Muhammad Hamza, Engr. Usman for always making time for us and guiding us throughout the project. Last but not the least we would also like to thank our friends and family for their cooperation and support.

ABSTRATCT

Thermal protection system (TPS) is an essential component of the space vehicles to protect them against the aerothermal heating that takes place during atmospheric entry. With time the demand for reusable launch vehicles (RLV) is increasing hence the pursuit for developing effective TPS has been accelerated. So in order to provide protection to the vehicles a porous ceramic foam tile consisting of silica (Si02) has been prepared. The tile was prepared by ultra-sonication, filtering, pressing and subsequent sintering. Numerous samples were prepared, and different parameters were changed to optimize the dispersion of the fibers in order to achieve maximum porosity and low values of thermal conductivity in the sample tile. Observations about dispersion of fibers in the tile was made after analyzing the microstructure using SEM images. Characterization of the tiles using BET determined the surface area, thermal conductivity test determined the change in thermal conductivity with porosity and compression testing determined the strength of these ties. The results were then compared with the already manufactured tiles already being used for thermal insulation system as reference and analysis was done.

Table of Contents

LIST OF FIGURES

LIST OF TABLES

CHAPTER 1

INTRODUCTION

1.1 THERMAL PROTECTION SYSTEM

Thermal protection system is a set of ceramic matrix composite tiles which are used to protect the space shuttle from high temperatures reached during reentry. When a space craft has to return to earth after completing its mission, it is travelling at a hypersonic speed. The spacecraft compresses the air in front of it and a shock wave is created due to which the temperature can rise to as high as 3000° F during reentry and this excess heat is detrimental for space crafts. The reason is the structure of a spacecraft which is made up of metals like Aluminum and stainless Steel.

Aluminum is usually preferred due to its light weight. However, Aluminum can survive temperature as high as 1221°F. Beyond this temperature, Aluminum metal and its alloys will melt. Stainless Steel on other hand melts at 2500 - 2785 °F. The temperature during reentry can reach up to 3000° F and the metals that make the outer structure of the spacecraft will melt during re-entry. For this purpose, a thermal protection system is required which consists of a set of tiles is that will provide insulation to the space craft's outer body against the high heat during reentry.

1.2 Types of Thermal Protection System

The TPS is of two types i.e. Ablative Thermal Protection System and Insulative Thermal Protection System. TPS consists of seven types of tiles which cover the entire spacecraft. These seven types of tiles are as follow

1. High temperature reusable surface insulation (HRSI) tiles
2. Low temperature reusable surface insulation (LRSI) tiles

3. Reinforced carbon

4. Flexible Insulation blanket (FIB)

5. Toughened uni-piece fiber insulation (TUFI)

6. Fibrous refractory composite insulation (FRCI)

7. Felt reusable surface insulation (FRSI)

1.3 Ablative Thermal Protection System

As the name suggests, these tiles are made from ablative materials. Ablative materials are those materials which degrade or pyrolyze when they are exposed to high temperature. Some examples of these materials are carbon carbon composites, resin, aluminum oxide, silicate, composite of silica fibers reinforced phenolic matrix etc. [7]. Ablative materials are sacrificial materials that protect the structure of spacecraft by degrading or pyrolyzing when exposed to high temperatures of reentry. Ablative materials used for thermal protection system can be both polymeric and non-polymeric. Polymeric ablative materials are the most widely used ablative materials in spacecraft because they have certain advantages over non polymeric ablative materials; they are cheaper, and they provide better resistance to high temperatures reached during reentry [7].

When ablative TPS tiles are exposed to reentry heat, they undergo ablation process i.e. they pyrolyze and reject heat by pyrolysis of polymer. [8]

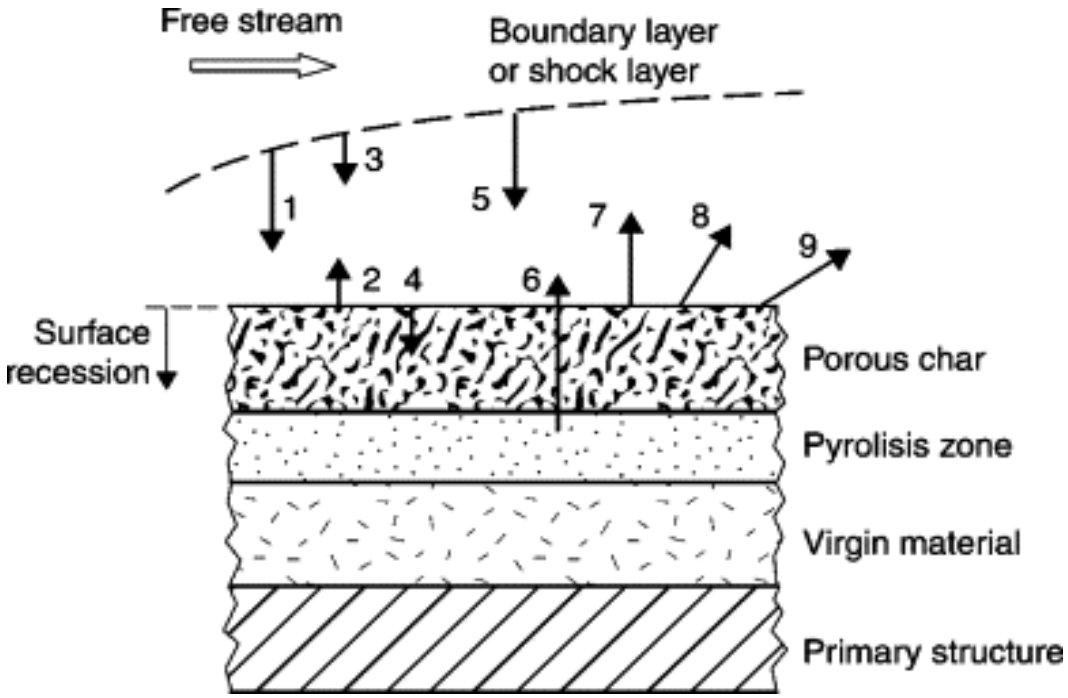

Figure 1 Ablation of a material [18]

The process of ablation involves rejection of reentry heat by material loss. Thus, ablative TPS tiles are non- reusable. After every flight, new set of tiles have to be installed before the space craft can take off for next mission. The ablative material will protect spacecraft from reentry heat in 3 ways [9];

1. Pyrolysis of ablative material.

2. Melting of ablative material.

3. Sublimation of ablative material.

A typical ablative thermal protection system consists of 4 layers. At the very bottom is the primary structure, upon which is the virgin material guarded by pyrolysis zone and above pyrolysis zone is the porous char. Outside this porous char, is the steam.

1.3.1 Properties of Ablative thermal protection systems

1. An ablative TPS material should have high value of heat of ablation. High heat of ablation means that less weight of material will be required to accommodate incoming heat [10].
2. An ablative material should have high mechanical strength in order to survive the forces faces during reentry [10].
3. t should have low thermal conductivity. This is because heat shouldn't be allowed to reach the metallic structure beneath ablative tile [10].
4. Ablating temperature should be high so that the material loss takes place only at very high temperatures [10].
5. Thermal properties include thermal conductivity and specific heat, physical properties include density and hardness of the tile and mechanical properties include strength, toughness and modulus of elasticity [8]

1.3.2 Types and Classification of Ablative TPS

Ablative TPS are usually classified into high density, mid density and low density ablative TPS. As density of ablative material increases, the mechanical strength also increases. But the thermal conductivity decreases with increasing density [9]. Based on method of fabrication, Ablative TPS are classified as rigid, conformable, woven and flexible [8]. Rigid ablative TPS are manufactured in rigid form and attached to a rigid substrate. Conformable ablative TPS are manufactured in flexible form and attached to a rigid substrate. Flexible ablative TPS are manufactured in flexible form. Comfortable and flexible ablative TPS are made from various resins and fillers. Woven ablative tops are made by weaving fibers in a 3d manner and then resin transfer molding is done.

1.3.3 Reinforced Carbon -Carbon Composite

Reinforced carbon-carbon is an ablative TPS material which is a graphite matrix composite reinforced with phenol resin. It is used on the nose cap and leading edges

of wings[11].

For making this ablative TPS material, graphite is cured in autoclave and impregnated with phenol resin as reinforcement. Then pyrolysis is done to convert phenol resin to carbon. Then mechanical properties are enhanced by increasing density. This is done by adding fur-furyl alcohol in vacuum chamber and pyrolyzing. This process is repeated 3 times. Fur-furyl alcohol consists of furan group [11]. A shortcoming of carbon is that it oxidizes at

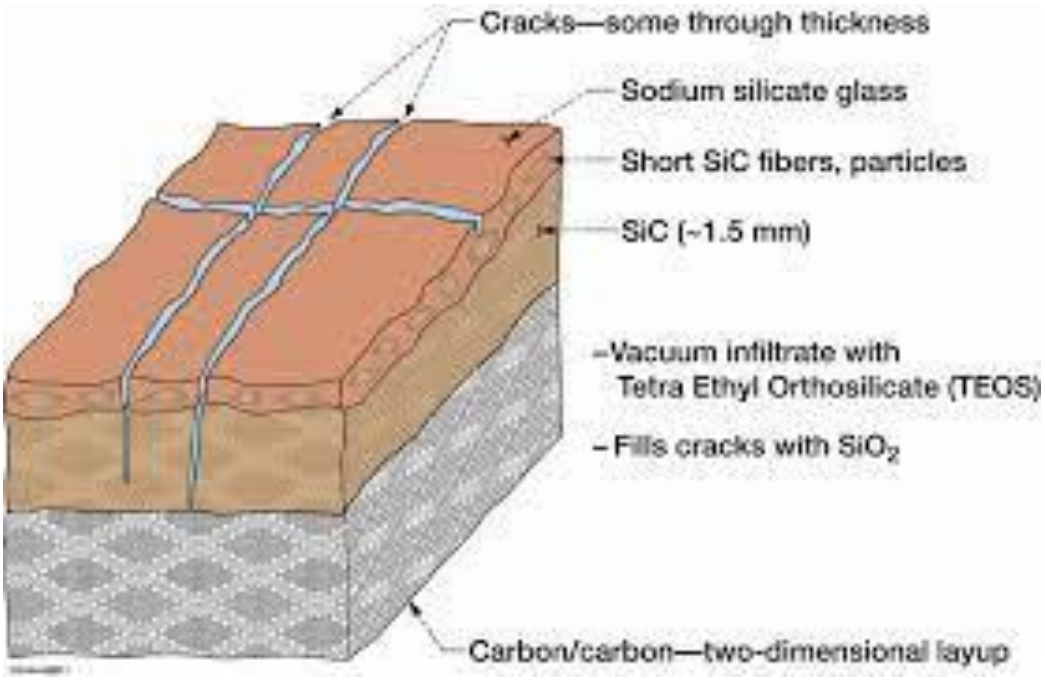

Figure 2 Reinforced Carbon-Carbon Composite [19]

high temperatures reached during reentry. Oxidation of carbon will have adverse effects on strength of the ablative tile. To prevent oxidation of carbon at high temperatures, it is coated with SiC. Reinforced carbon-carbon removes heat by two phenomena known as external radiation and cross radiation. External radiation means that the reinforced carbon-carbon will take heat from the surface and reject it into surrounding. On the other hand, cross radiation refers to the transfer of heat between layers of reinforced carbon-carbon [11]. A shortcoming of reinforced carbon-carbon ablative TPS tile is that it has high thermal conductivity. So it cannot

effectively resist the reentry heat from reaching metallic structure of spacecraft [11]. It has low thermal conductivity but goof mechanical strength. Reinforced carbon-carbon ablative TPS tile can endure up to 2,700° F. The density of carbon-carbon reinforced ablative TPS ranges from 1.45 - 1.5 g/cm^3.

1.3.4 Advantages of Ablative Thermal Protection System

Some advantages of ablative TPS are as follow.

1. Ablative tps provides resistance to high temperatures reached during reentry [10].

2. Design of ablative TPS materials are simple and flexible [10].

3. Polymeric ablative TPS materials are cheaper [10].

1.3.5 Disadvantages of Ablative Thermal Protection System

Some disadvantaged of Ablative TPS are

1. Non- reusable due to material loss

2. Mechanical strength is not very good.

3. Life of material is time dependent [10].

4. Due to mechanical stress, a phenomenon called char spallation takes place which is a type of erosion. As a result of this phenomenon, some mass can become detached from surface of spacecraft [9].

1.4 Insulative Thermal Protection System

Insulative TPS is made from insulative materials which have very low thermal conductivity and are able to withstand high temperatures reached during reentry. These materials either absorb or reject heat and thus protect the space craft from damage due to reentry heat. Silica is the most widely used material in this application.

This is because of its low thermal conductivity. There are several types of insulative tiles which cover the surface of spacecraft. Each part of space craft has a particular type of tile depending on the temperature and mechanical stress faced by this portion. Now we will look at these different types of Insulative TPS tiles.

1.4.1 High Temperature Reusable Surface Insulation Tiles (HRSI)

As the name suggests, these tiles are used on areas where high temperatures are faced. These tile cover areas where temperature is up to 1260°C. These tiles have high mechanical strength, so they cover regions like landing gear doors etc. where high mechanical stress is required. The HRSI tiles are of two types. LI-900 and AETB-800. These tiles are foam like and white in color. The space shuttle consisted of over 20,000 HRSI tiles. The underside or belly of space shuttle was entirely covered with these tiles. When spacecraft descends, it is at such an inclined angle that the belly of space craft is directly facing towards earth and the temperature is very high. HRSI tiles are coated with black coating of reaction cured glass made from borosilicate. These rcc coatings enhance the heat sink properties of HRSI. About 95% of the heat is rejected by rcc coating and remaining 5% is absorbed by the ceramic foam HRSI tile. In this way the metal beneath the tile is protected from high heat of reentry.

1.4.2 Toughened Uni-piece Fiber Insulation (TUFI)

As the name suggests, TUFI is a very tough tile. These tiles are black in color and cover underside and upper body. It has two versions. High temperature version and low temperature version. The high temperature version is black in color and low temperature version is white in color. While black tiles have better insulation, white tiles are lighter. These tiles provide better toughness and impact resistance, but thermal insulation is compromised.

1.4.3 Felt Reusable Surface Insulation (FRSI)

Like TUFI, FRSI, also provides good toughness. It is used at parts where temperature is between 300 to 700°C. It provides good toughness, impact resistance, cracking resistance and also lighter weight.

1.4.4 Advantages of Insulative TPS over Ablative TPS

Insulative TPS has some advantages over ablative tps which are discussed below.

1. First of all, the ablative tiles are not reusable due to the material loss as the material pyrolyzes during reentry. After every mission, new tiles have to be installed. On the other hand, Insulative tiles are reusable, and they don't decompose due to high temperatures during reentry. The insulative tiles can be reused for future missions and only have to be replaced when a tile takes physical damage.
2. Insulative tiles are more cost efficient as compared to ablative tiles. The cost of an installed square foot of reusable tile, which can be used for up to 100 missions, cost NASA around $10,000. Whereas, per square foot cost of the ablative tiles which were used on the Apollo mission's module costs around $30,000. In fact, for every mission, new tiles worth $30,000/ square foot had to be installed [12].
3. Insulative tiles are much lighter than Ablative tiles [13].
4. Ablative tiles are much more fragile as compared to insulative tiles, due to the low density of ablative materials [13].

1.5 Applications of Thermal Protection System

Space shuttle descends at an angle of 40°. In this position the areas that face the most heat are the belly of space shuttle and leading edges i.e. the nose wings. Other areas also face high temperatures, but they are covered with different type of tiles. The variety of tiles not only depends on temperature but also on the mechanical strength. For example, tiles near landing gear will require higher mechanical strength.

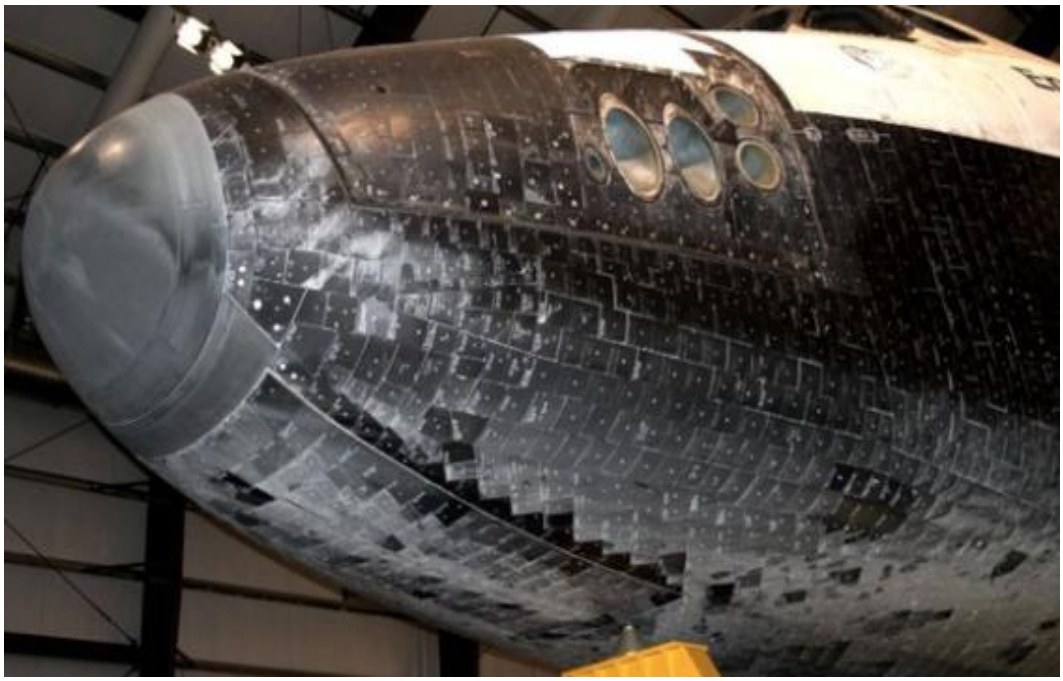

Figure 3 Application of TPS at nose cap and belly of space shuttle [17]

1.6 Bonding of Tiles to the space craft's surface

The tiles can be attached by using some adhesives or by riveting. The adhesives used by Nasa are silicone adhesive and Viton adhesive. Silicone adhesive shows excellent bond strength at high temperatures during reentry. Viton adhesives also possess good temperature and chemic resistance. Viton adhesives are made from flour elastomers. Now, Elon Musk's space X is joining the tiles to starship surface through riveting. An advantage of riveting is that the disassembly of tiles is much more efficient as compared to the glued tiles. There are thousands of tiles on a space craft's surface and each tile is given a specific code. In this way it is easier for space agencies to identify the location of tile which needs maintenance.

CHAPTER 2

LITERATURE REVIEW

2.1 Re Entry Heating

When a space craft takes off from earth, it moves with aid of rocket engines that carry it into the outer space. But when the space craft has to return to earth after completing its mission, it doesn't move with help of engines, rather it is falling under the action of earth's gravity. During this fall, the space craft is travelling at a high hypersonic speed of 25 Mach, which turns out to be 8575 m/s. As we know that things which go faster, tend to become hotter, the temperature of space craft is very high during the atmospheric reentry. Moreover, a space craft entering earth's atmosphere faces atmospheric drag and aerodynamic heating. Atmospheric drag is responsible for the mechanical stress faced by space craft. The drag increases as altitude lowers. Aerodynamic heating on the other hand results in increase temperature due to flow of gases over space craft resulting from compression of air. The temperature can rise to as high as 3000° F.

2.1.1 Sources of Reentry heating

When a spacecraft enters earth's atmosphere with such high velocity of Mach 25, it will face high levels of heating which can be dangerous for it. The sources of this heating are as follow; [1]

1. Convective Heating: Convective heating is caused by flow of hot gases past the spacecraft and due to chemical reactions between these gases and the spacecraft's body [1].
2. Radiative Heating: Due to high supersonic speed of spacecraft, a shock wave is established in front of the spacecraft. This shock wave causes radiative heating when air gets ionized due to high temperature. [1

More than 80% of the heat faced by space craft is due to compression of hot gases present in front of it. We can explain this by Gay Lussac's Law which formulates a relation between temperature and pressure. According to Gay Lussac's law, "At a given amount of volume, the pressure of a gas is directly proportional to the temperature".

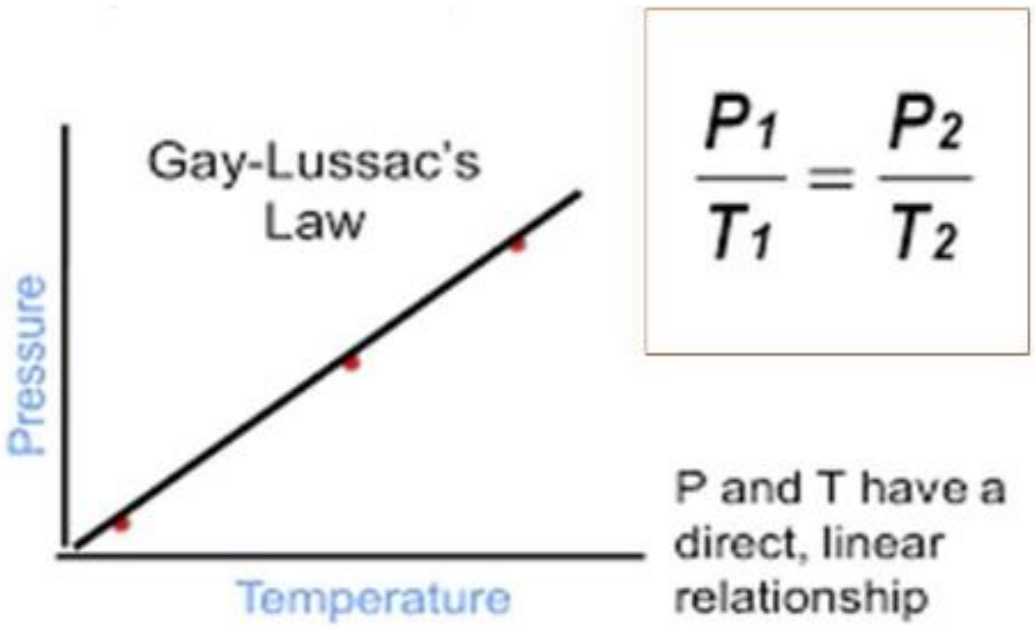

Figure 4: Gay Loussac's Law [15]

Thus, this law leads us to the conclusion that, more the pressure due to compression of gases in front of spacecraft, higher will be the temperature reached.

When an object moves at a supersonic or higher speeds, a shockwave is created in front of it. Like other forms of waves, shock wave carries some energy, and it can also propagate through mediums, but it causes abrupt changes in pressure and temperature of the medium [2]. Shockwaves travel faster than sound and if the amplitude increases, the velocity also increases. The shock wave not only increases temperature, but it also protects the surface of spacecraft from direct contact with heat, which can be very dangerous. A shockwave does so by deflecting most of the

heat. So radiative heating has lesser effect than convective heating [3] . In convective heating, hot gases pass through the shock front. Shock front serves as the boundary beyond which, a body faces changes in its physical conditions due to shock wave. When gases travel through this shock wave, they are ionized to superheated plasma. Suffice it to say, that most of the reentry heating is due to this superheated plasma [3] . This superheated plasma is formed when electrons are ripped away from atoms. For superheated plasma to form, the gas has to be superheated first. Shockwave created during reentry, due to radiative heating, provides this high temperature. The temperature of plasma can range from 11,000 - 14,500 °F.

Both sources of reentry heating i.e. convective heating and radiative heating increase as the speed of space craft increases. At early stages of reentry, radiative heating dominates and at later stages convective heating dominates. [1]

2.1.2 Effect of Re Entry Heat on Spacecraft:

We have already discussed the reasons for high temperature reached during reentry. Now we will look at why this heat is dangerous for spacecraft.

The structure of a spacecraft is made of metals like Aluminum and stainless Steel. Aluminum is usually preferred due to its light weight. However, Aluminum can survive temperature as high as 12, 21°F. Beyond this temperature, Aluminum metal and its alloys will melt. Stainless Steel on other hand melts at 2500 - 2785 °F. The temperature during reentry can reach up to 3000° F and it is apparent that the metals used for outer structures of spacecraft will melt and cause destruction of the spacecraft.

Moreover, if the hot gases come in contact with metallic structure, they can penetrate and cause problems for space craft, as happened with the Columbia space shuttle in 2003.

Figure5: An orbiter undergoing atmospheric re-entry [16]

2.2 The Columbia Disaster

Columbia disaster took place on February 1st, 2003. The Columbia space shuttle was making its reentry on this date after completing its mission. During takeoff, one of the polyurethane insulation foams from the fuel tanks had broken off and hit the Carbon-Carbon reinforced tile on wings, therefore exposing some portion of wings. When Columbia attempted its reentry, this exposed portion of wings came in direct contact with the hot gases. These hot gases penetrated into the wings and destroyed them, as a result the space shuttle became unstable, and the crown witnessed space shuttle Columbia disintegrating over central Texas. This incident shows the importance of shielding metallic surface of spacecraft from the reentry heat [4].

In light of above difficulties imposed by reentry heating, a heat shielding mechanism is necessary for space crafts to have a safe landing. This heat shielding is provided by the Thermal Protection System (TPS)

2.3 Thermal Protection System

Thermal protection system is basically a set of different tiles which are used to protect the space shuttle from adverse effects of reentry heating. Theses tiles are mostly made of ceramic matrix composites. TPS tiles are not attached directly to the metallic body of space shuttle, but they are first attached to Nomex pads which are then attached to the metallic structure. The Nomex pad provides flexibility to the brittle tiles. Nomex is a textile aramid fiber and is made mostly of nylon. It possesses high mechanical toughness, resilience, thermal stability and flexibility. Nomex is also insulating so it provides resistance, and it is also chemically stable. The TPS tiled are attached to Nomex blanket via silicon adhesive. However, a spacecraft consists of thousands of tiles and applying glue to every single tile is time consuming. A new strategy being adopted by Space X is riveting the tiles rather than applying glue.

TPS tiles are excellent insulators of heat. If a person holds tile by one end, and heat is applied to the opposite end, the person will not be able to feel heat even if the tile was red hot on opposite end [5].

The main selection criteria for TPS tiles is [6];

1. Light weight

2. Low thermal conductivity

3. Good mechanical strength

In some areas of space shuttle, where more impact resistance was needed, a heavier type of tile was used [6]. TPS consists of a number of different types of tiles. This variety of tiles is based on the area of application. This is because some parts of space shuttle will encounter higher temperature than the rest.

Tiles being used the most for thermal protection system are listed below. The raw materials used to make these tiles and their properties are discussed below.

2.3.1 Lockheed Insulation 900 (LI-900)

Lockheed Insulation materials include high purity of amorphous Silica fiber. For its production, Silica fibers with a diameter of 1 to 3 um mixed with ionized water in a V-blender and formed into slurry. The slurry is mixed with ammonia once stabilized colloidal Silica Solution after that, is added and water is drained and slightly pressed into it to remove remaining. Slightly dry slurry is heated to a temperature of 250°F to remove any remaining water. Slurry is dried and then sintered at temperature of up to 2300° F. The resulting protective material is low density silica fibers that are randomly dispersed. Li-900 has very low thermal conductivity. RCC glass is applied on these tiles. These RCC coating will reject the heat during reentry. The major disadvantages of Lockheed Insulation 900 are the low strength of silica fibers and shrinkage at high temperatures. Silica fibers undergo shrinkage above 2500°F. Due to low mechanical strength, Li 900 tiles are susceptible to damage [14].

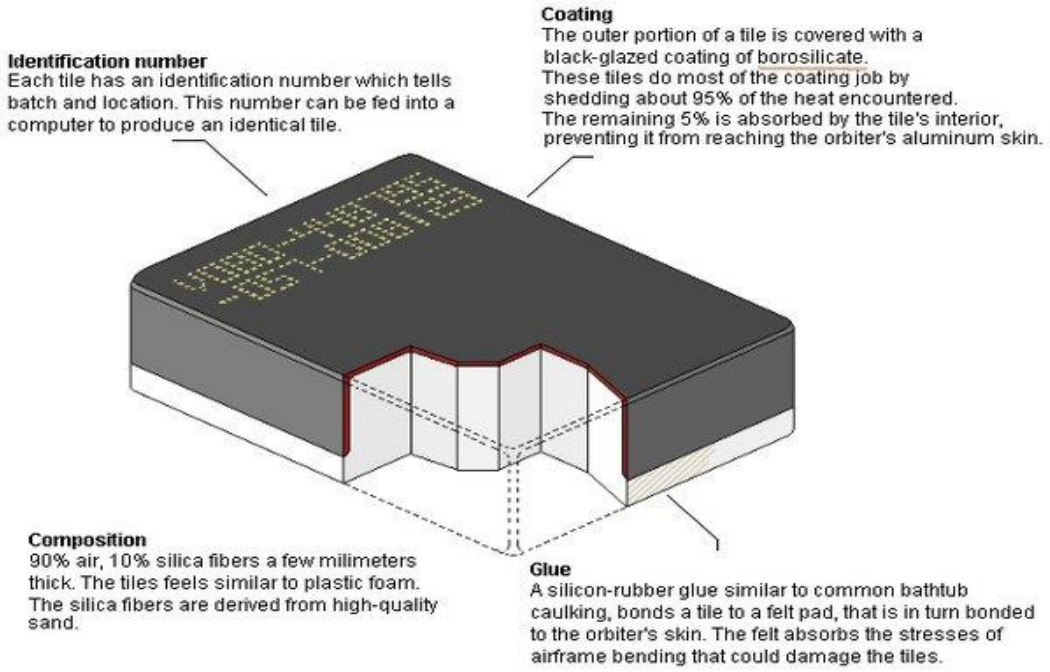

Figure 6 Lockheed Insulation 900 (li-900) tile [20]

2.3.2 Alumina Enhanced Thermal Barrier (AETB)

AETB is another type of HRSI. These are similar to Li-900 with the exception that these are made from Alumina fibers rather than Silica fibers. Like Li 900, AETB also have foam like appearance. These tiles consist of, 68% Silica fibers, 12% Nextel Fibers, 20 percent Alumina fibers and 2 percent binder. The Nextel fibers are a combination of Al2O3 and SiO2 fibers. Their diameter is around 5 mm. The binder used is a ceramic carbide or nitride like Boron nitride. Binders when heated to high temperature during sintering, fuse together the fibers. Sintering is done at 1200-1300 °C. AETB is basically a modification of Li-900. Alumina fibers are added to enhance strength. But as a result of this modification, the thermal conductivity is compromised since alumina fibers have higher thermal conductivity then silica fibers. For this reason, the use of AETB is very restricted and it is used at those areas where heat is lower as compared to areas where Li900 is used [14].

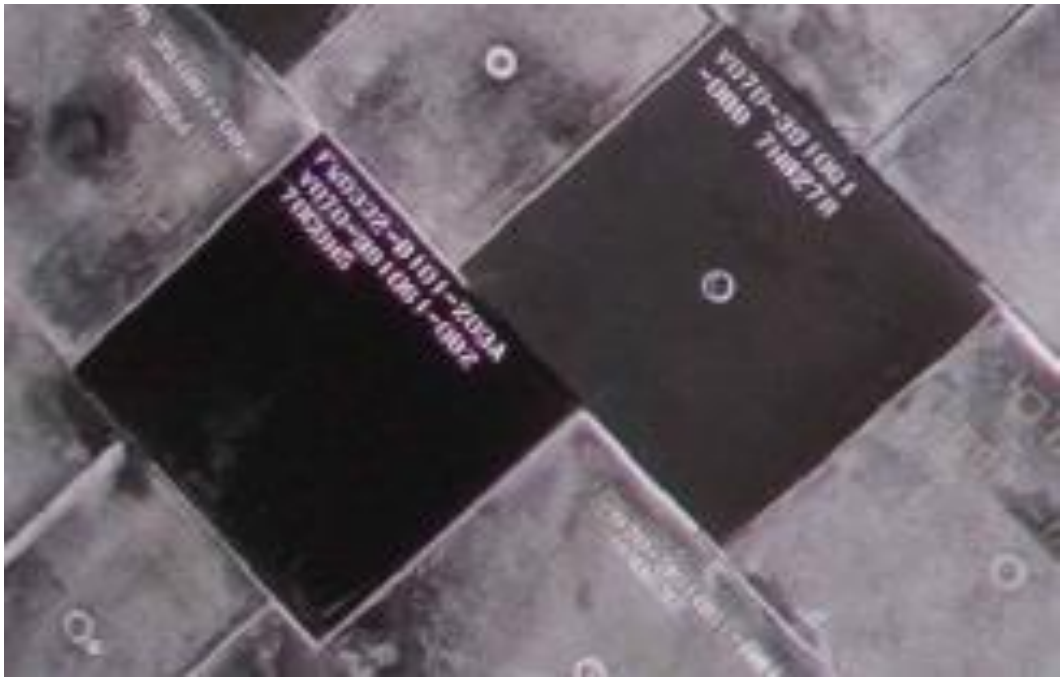

Figure 7 Alumina Enhanced Thermal Barrier (AETB) tile [21]

Both LI-900 and AETB have similar manufacturing methods. First of all, the fibers are

mixed with Deionized water, binder and Surfactant. 60-80% Silica fibers, 20-40% Alumina fiber and 0.1-1% binder are added. The ceramic fibers are dispersed in de ionized water solution to form a slurry. A shear mixer is used to blend this slurry. After slurry is formed, and fibers are well dispersed, the inclusions or impurities are removed. These impurities can have adverse effects on properties and also add to the overall weight of tile. These inclusions can also prevent desired porosity. High density inclusions are also detrimental to the thermal resistance of tile. The inclusions are removed through filtration. Once the inclusions are removed, the slurry is pressed into billets. Pressing is done through hydraulic pressing. Then water is drained from these pressed billets by gravity sedimentation or vacuum filtration. Then the billet is heated in an oven at about 200-500°C for a whole day. After removal of water the billet is sintered at 1200-1300°C. During sintering, the fibers are fused together. During drying and sintering, the gap should not be more than 1 hour because the billet might absorb moisture and result in cracking during sintering. During sintering the boron carbide or boron nitride binding agent, decompose to borated. These borates fuse together the fibers. After sintering the tile is ready for machining. Final dimensions of a ceramic foam tile block are 6"x6"x2". The geometry of tile can be altered to fix it at different areas of spacecraft. The density of a finished tile is about 8 lb. /ft^3 [14].

2.3.3 Low Temperature Reusable Surface Insulation tiles (LRSI)

These cover the upper wing close to the main edge. These tiles protect regions where reentry temperatures are under 1,200 °F (649 °C). The LRSI tiles are made in a similar way as the HRSI tiles, then again, actually the tiles are 8 by 8 inches (20 by 20 cm) squares and have a white RCC glass coating made of silica and alumina. These tiles are reusable for up to 100 missions [13]. The dimensions of LRSI tiles are 7.5"x9"x3/4". There were about 7000 LRSI tiles on Space shuttle. These tiles covered the tail, upper wings and fuselage.

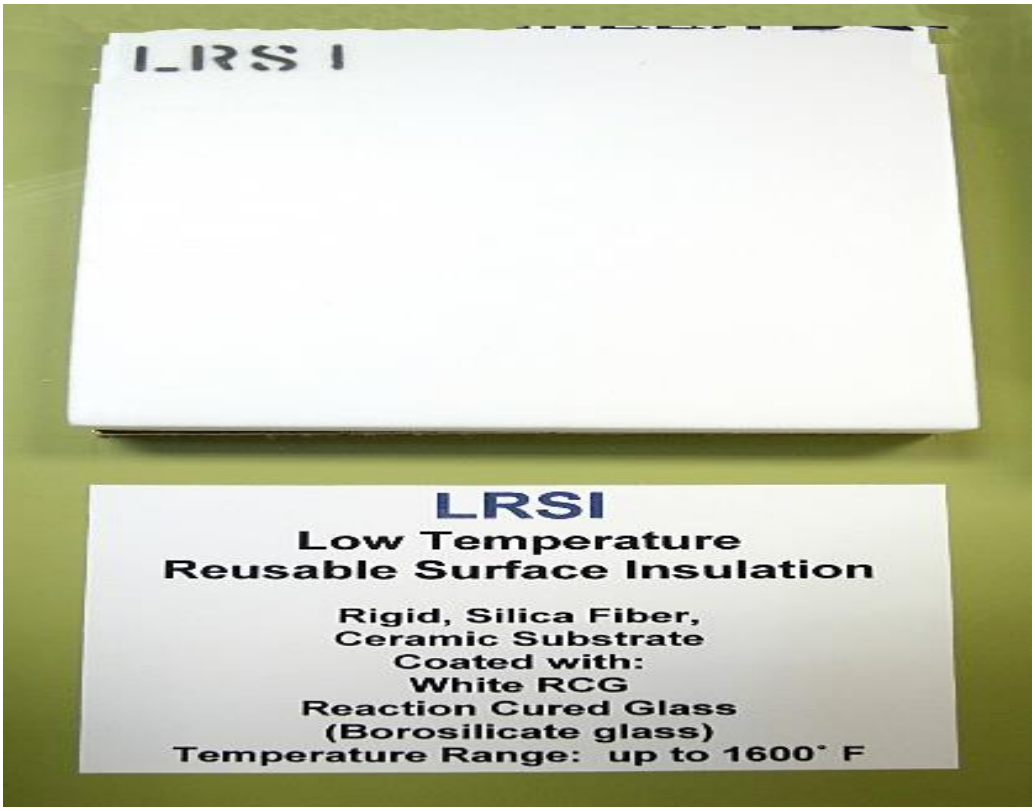

Figure 8 LRSI tile

CHAPTER 3

METHODOLOGY AND CHARACTERIZATION

3.1 Solution Preparation:

The first step in the manufacture of these tiles is solution preparation, the raw materials that we have are:

- Silica fibers (2-3 μm diameter)
- Binder (boron oxide)
- Surfactant (TX-100)
- Distilled water
- NaOH pellets
- Hcl solution

In distilled water 0.5 to 1 gram of NaOH and HCL 1 to 2 drops were added to adjust the solutions pH values from 9 to 10. Once the pH is set than about 0.1 weight percent to 1 weight percent boron oxide powder is added followed by 1 to 2 drops of surfactant i.e. (TX-1OO) in the solution. The solution is magnetically stirred so that all the ingredients are uniformly mixed in the solution. The silica fibers ae scrutinized to remove any clumps of fibers after which the fibers are added to the solution. These fibers are added according to fiber to water ratio of 1 g: 47 ml, while the solution is still being stirred magnetically. The speed of stirring is around 200-500 revs per minute so that the fibers are stirred uniformly in the solution without settling down at the bottom. Here the speed of mixing is a very critical factor, if the speed is too high the fibers will start to make shots or clumps of fibers and the foremost objective is to prevent this agglomeration of fibers.

3.2 Ultra-sonication:

The ultra-sonication is a process to agitate the particles present in solution by using sound waves. When ultrasonic waves pass through a liquid medium, a large number of micro bubbles form, grow and collapse due to alternate high and low pressures. The purpose of doing ultra-sonication is to obtain a colloidal solution of the fibers. The process is done in a water bath sonication that works normally on 30K to 40K frequency. The beaker containing the solution is placed in the bath sonication and the start button is turned on. The ultra-sonication is done for 2-6 hours normally.

Ultra-sonication disperses the fibers in the in-plane direction (perpendicular to the pressing direction) by the radial flow of the water through ultrasonic waves. This directional arrangement of fibers results in much lower conductivity in through the thickness direction as compared to the in-plane direction. Ultra-sonication has a positive co-relation with the dispersion of fibers.

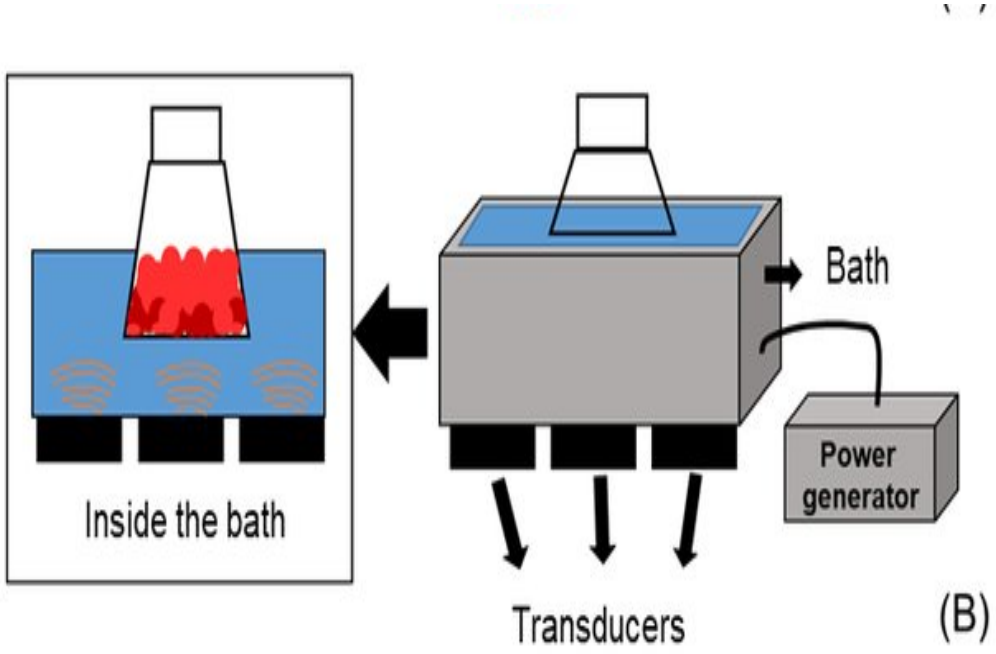

Figure 9: bath ultraonication equipment used to diperse the fibers. [23]

The figure below shows image of the the solution after ultra-sonication.

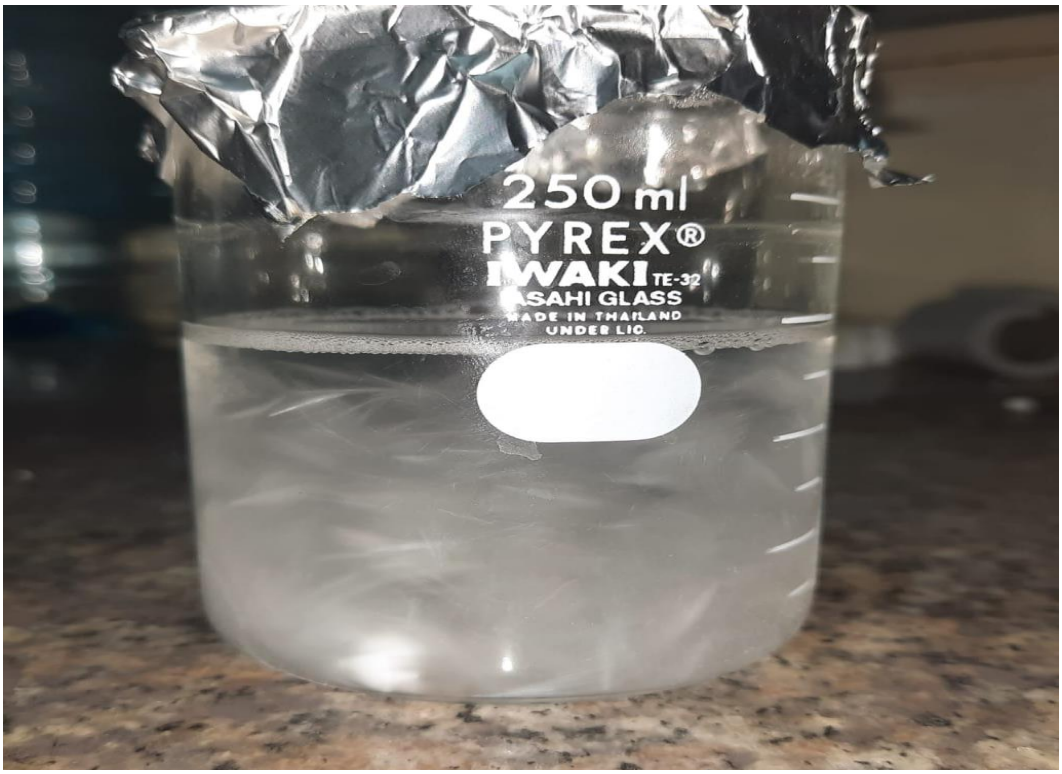

Figure 10: Solution of silica fibers dispersed right after ultra-sonication for 5 -6 hours.

3.3 Mechanical Stirring:

Mechanical stirrer is used for stirring after ultra-sonication as the fibers after sometime settle at bottom in the form of a single layer. Stirrer breaks the fiber layer so that the fibers can again remain dispersed in the sample before filtration is done. Mechanically stirring chops the layer of fibers resulting in the formation of small dispersed lumps which are removed when the solution is ultra-sonicated the second time. Mechanical stirring is done for only 2-3 minutes at a low velocity to avoid breakage of fibers. Extra care is taken to ensure that length of the fibers isn't reduced as it effects the mechanical properties. There's no effect of mechanically

stirring on the diameter of the fibers. Stirring velocity is the most critical factor here. If it is too low, the layer will not be broken down, if it is too high, the fibers will break down individually.

3.4 Filtration:

Filtration is done by using a modification of drain- gravity method in which insoluble silica fibers are separated from the water solution by the action of gravity. The purpose of filtration is to have a wet billet at the bottom of the apparatus with dimensions similar with the dimensions of the billet to be reduced. But due unavailability of exact filter die, the exact dimensions were not achieved. The apparatus used for this purpose was a porous funnel 10 cm diameter and a nylon paper of pore size 0.3 μm and a diameter of 45 mm. Filtration was normally done overnight so that all the water content could be filtered out from the fibers and the fibers get dry simultaneously.

Figure 11: porous funnel used for filtration by gravity sedimentation method.

3.5 Hydraulic Pressing:

Hydraulic pressing was done in metallic die of 3 mm diameter providing the tile thickness of 3 mm. It was done using a hydraulic press. The pressure applied was around 40- 60 psi and the time taken was around 2-3 minutes. The hydraulic pressure and pressing time are critical factors in this operation because the fibers can be damaged by higher pressures causing impediment to the thermal conductivity.

FIGURE 12: HYDRAULIC PRESS MACHINE

3.6 SINTERING

After the green compact is formed, sintering is done to achieve densification which required to give adequate strength to tile. Sintering was done using a Muffle Furnace at a temperature of 1200-1300 Celsius with a ramp rate of 10 degree per minute 3-5 hours. There are two critical factors in this operation:

3.6.1 Sintering Time

Sintering Time is directly proportional to densification and to achieve the desired bulk density of 8 lbs. $/ft^3$ to 20 lbs. $/ft^3$ and percentage porosity of 80-90 percent 3-5 hours should be used. If excess time is given the sample may have agglomerations, if the sample is not sintered for long enough it may lack structural integrity.

3.6.2 Sintering Temperature:

Sintering Temperature is also directly proportional to densification but also acts as the activator for necking and the sintering process. To achieve the above-mentioned densification and porosity an optimized temperature of 1200°C to 1300°C should be used. If the temperature is lower than specified; necking is insufficient leading to larger percentage porosity and lower structural integrity and if it is above the specified range; agglomerates start to form leading to greater values of thermal conductivity.

Figure 13: muffle furnace

Using the procedures mentioned above number of experiments were carried out and some parameters like (ultra-sonication time, mechanical stirring, and pressure) were changed and effects on microstructure are studied. The following table shows the variations that were done in different experiments and effects on microstructure are studied.

Table 1: showing different variations to optimizing the parameter

	Variation 1	**Variation 2**	**Variation 3**	**Variation 4**	**Variation 5**
Ultra-sonication	✓	✓	✓	✓	✓
Mechanical stirring	✓	✓	✓	✓	
Second ultra-sonication		✓	✓	✓	✓
Filtration	✓	✓	✓	✓	✓
Separating the fibers				✓	✓
pressing	✓		✓		
Sintering	✓	✓	✓	✓	✓
SEM analysis	✓	✓	✓	✓	✓

3.7 Testing:

3.7.1 Scanning Electron Microscopy:

SEM is performed to check the collective random dispersion of the fibers, individual orientation of the fibers which is approximately in the in-plane direction and subsequent necking from sintering between the fibers. The samples were prepared through paper cutting from the top and the bottom of the sintered tile. Image j software

was used to calculate the length and diameter of the fibers. SEM was done at magnifications ranging from 100X to 500X.

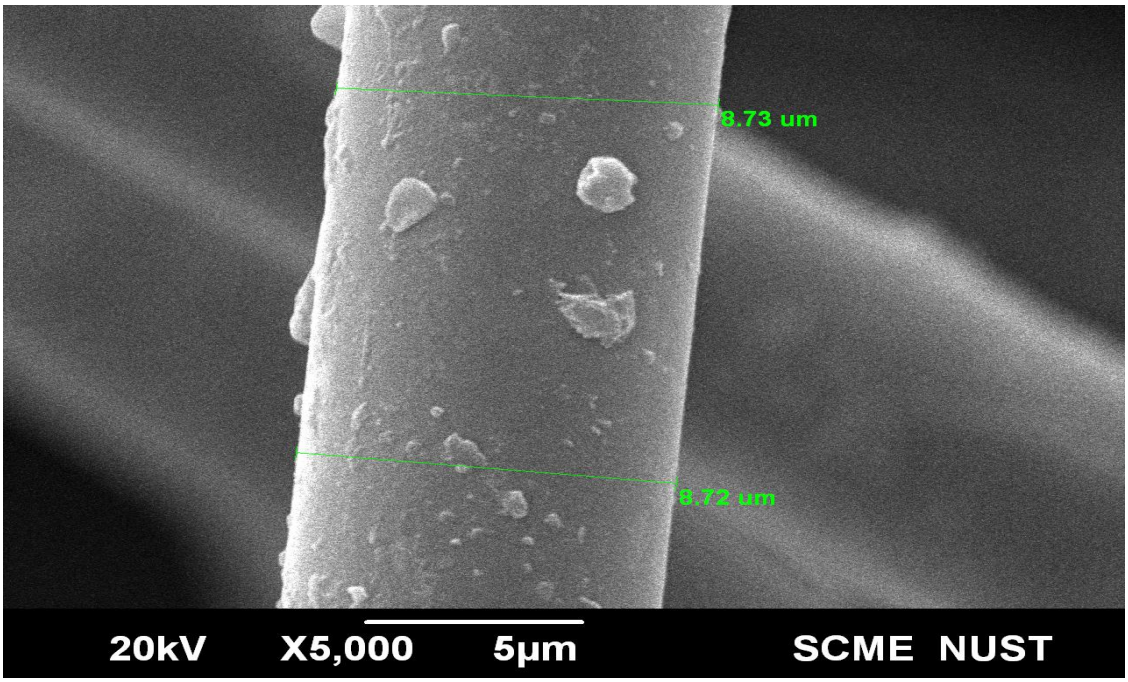

Figure 14: SEM image of raw silica fibers reporting diameter

3.7.2 Apparent porosity

Apparent porosity of the sample was calculated using Archimedes' principle. This method was used as the tiles isn't effected by water and the open pores of the tile are fully impregnated with water during weighing.

To calculate the first step is to weigh the dry tile (right after sintering) using electric weigh balance. The tile was then soaked in water and the weight was calculated while the tile was immersed in water. The tile was then removed from water the surface was bloated by smooth linen or cotton cloth to remove all water drops from the surface and the tile was weighed. Porosity is calculated by the formula mentioned below.

$$A = \frac{W_W - W_D}{W_W - W_S} \times 100$$

Where $W_w$weight of wet tile is, W_D is weight of dried tile and W_S is weight of tile after surface cleaning,

3.7.3 BET:

Brunauer-Emmett-Teller (BET) theory aims to explain the physical adsorption of gas molecules on a solid surface and serves as the basis for an important analysis technique for the measurement of the specific surface area of materials. A non-reactive gas is passed over the adsorb-ate such that the gas is physically adsorbed on the surface of the sample and the remaining gas molecules that do not react with surface are evacuated out of the chamber. The purpose of doing BET is to calculate the surface area of the sample, the pore size distribution determining the percentage porosity and make relationship between the specific surface area and the apparent porosity.

The apparatus used for BET analysis is HORIBA SA-9600. The degassing temperature was done for 2 hours at 110 °C. However, the manifold analyzer in the BET apparatus only measures the relative pressure of the gas during adsorption and desorption and the calculation of the surface area and the pore size distribution is done by the PC software.

Figure 15: BET apparatus

3.7.4 Thermal Conductivity Test:

After BET analysis, the samples were sent to NESCOM for thermal conductivity test. Many variations of methods and equipment are available to measure the thermal conductivity just like thermoelectric analyzer, Heat flow meter or Thermo-gravimetric. Thermal conductivity of solid materials was measured by guarded heat flow method by METTLER TOLEDO DSC3+ STAR SYSTEM according to the ASTM E1530 standard.

In guarded heat flow meter method, sample with 55mm diameter and 7mm thickness was placed between two surfaces, each controlled at different temperature under compressive load. An axial temperature gradient is established when heat flow from upper surface to the lower surface (part of calibrated heat flux transducer) through sample. Temperature difference can be measured by heat flux transducer, thickness and testing temperature is known; thermal conductivity of samples can easily be measured by employing one-dimensional Fourier's conduction law given by the equation:

$$Q = -\lambda A \frac{dT}{dx}$$

Where Q is the heat flux, A is the area, and -λ is the thermal conductivity.

It was observed that the samples with higher apparent percentage porosity had a lower value of thermal conductivity which was our main objective.

Figure 16: METTLER TOLEDO apparatus for thermal conductivity.

3.7.5 Compression Testing:

After thermal conductivity test, the samples were subjected to compression testing NESCOM. The compression test was performed to check the compression strength of the sample. The apparatus used for this purpose was MTS Sintech 10/GL according to ASTM D695 standard. The strain rate was 1mm/min during testing.

NESCOM provided us the data in tabulated form rather graphical form due to their closure policies. The compression strength mentioned above is basically the yield point of the samples. We couldn't observe the compression strength value of the first two samples because they didn't maintain their dimensions during the test because of high percentage porosity in the sample.

Figure 17: compression testing machine

CHAPTER 4

RESULTS AND DISCUSSION

4.1 SEM analysis and optimization

The main objective of our project was to ensure maximize dispersion of the fibers without the fibers breaking. A number of parameters were changed to find the best possible route that ensured maximum fiber dispersion. Then SEM images were used to analyze the microstructure, this was compared with literature and deductions about the dispersion of fibers in the sample were made. Whether dispersion was good or not was interpreted by spacing between the fibers in the SEM images as this porosity is required to obtain lower thermal conductivity. The SEM images were compared with those of li-900 and conclusion was drawn.

The silica fibers with a diameter of 2 to 3 microns and length approximately 117µm were used. The SEM image below shows the microstructure of raw silica fibers which was treated in different ways to maximize dispersion.

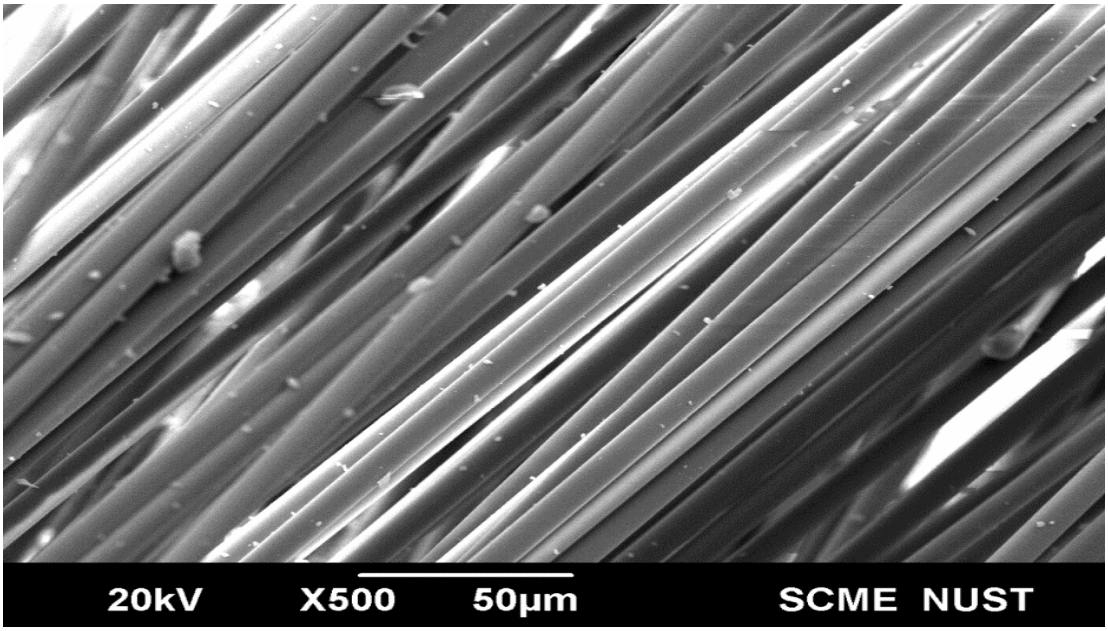

Figure 18: SEM image of raw silica fibers before any processing

4.1.1 Experiment 1

For variation 1 simple mechanically stirring of the silica fibers for 4 to 5 hours was done. The solution was then dried using a hot plate. The resulting fibers in the beaker were agglomerated together resulting in the formation of lump. This showed that simple mechanical stirring of the fibers was not the way forward.

Figure 18 shows the final condition of sample after the experiment. Lumps can be seen in it and this result was further confirmed by examining the SEM image (fig 19). It can be observed in the SEM images that the fibers are clumped together and further more they are broken because of the extensive mechanical stirring. The length of individual fibers is ranging from 84.09µm while the smallest fiber has a length of 23.71µm. Hence due to these smaller fibers agglomeration is more prevalent and it can be observed in the SEM image below.

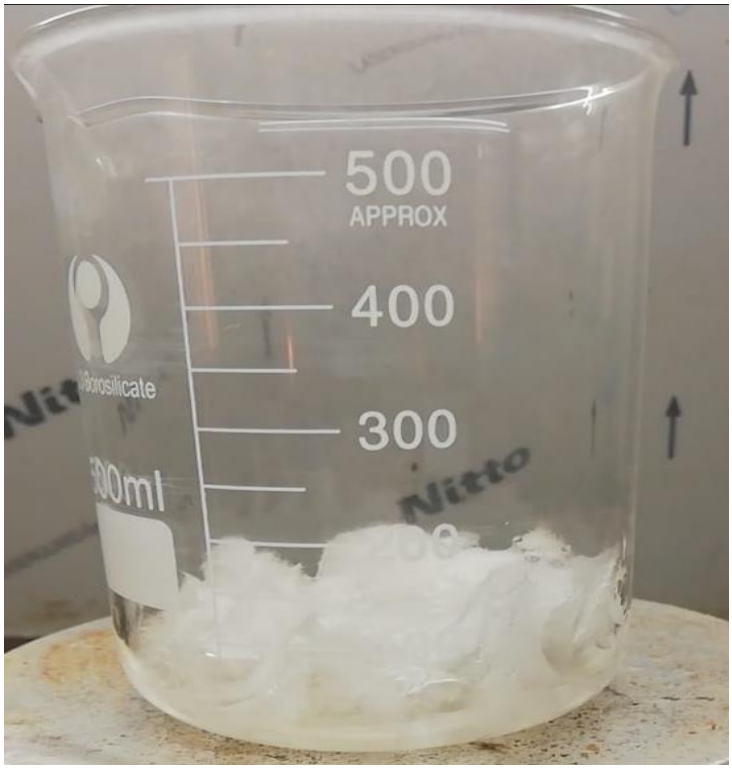

Figure 19: End product after experiment 1

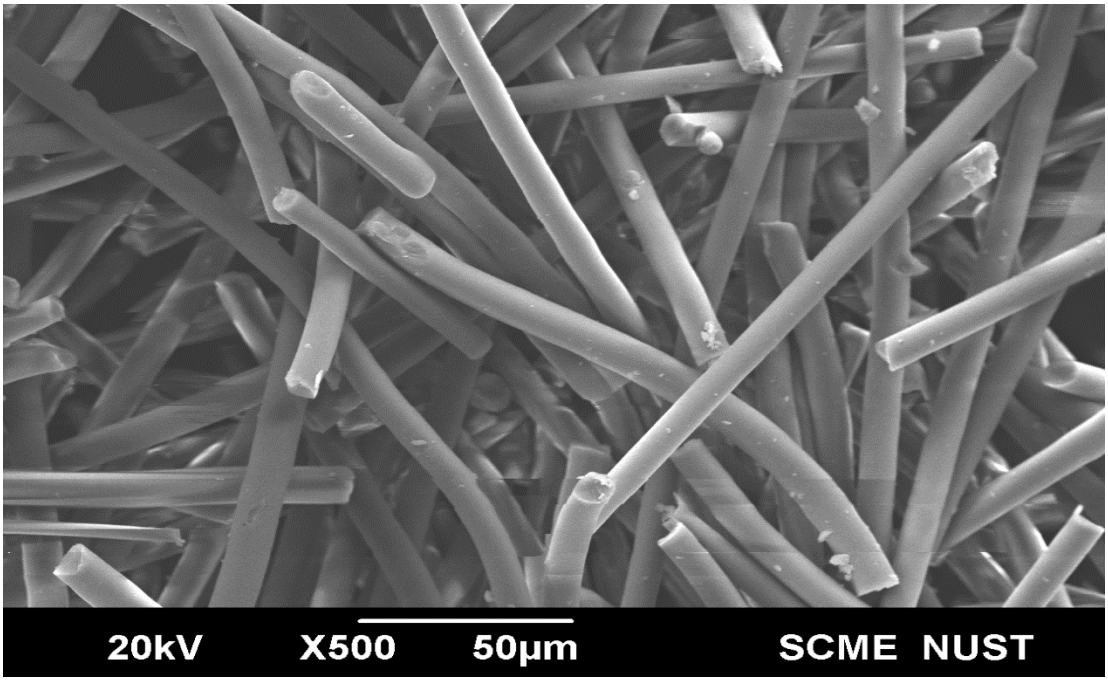

Figure 20: SEM image of sample tile of experiment 1

4.1.2 Experiment 2

In experiment 2 silica fibers ultra-sonication was done for 5 to 6 hours in order to achieve the required dispersion. After ultra-sonication the fibers were settled at the bottom of the beaker in the form of a single layer. This formation of single layer is also not it results in reduced dispersion hence maximum porosity cannot be achieved and neither lower thermal conductivity. The solution was then dried on a hot plate and a single layer of silica fibers was obtained where still some clumped fibers were present. This observation was further confirmed by the SEM images (fig 21 and 22) where we could observe spacing between individual fibers followed by some of the fibers also clattered together.

Figure 21: End product of experiment 2

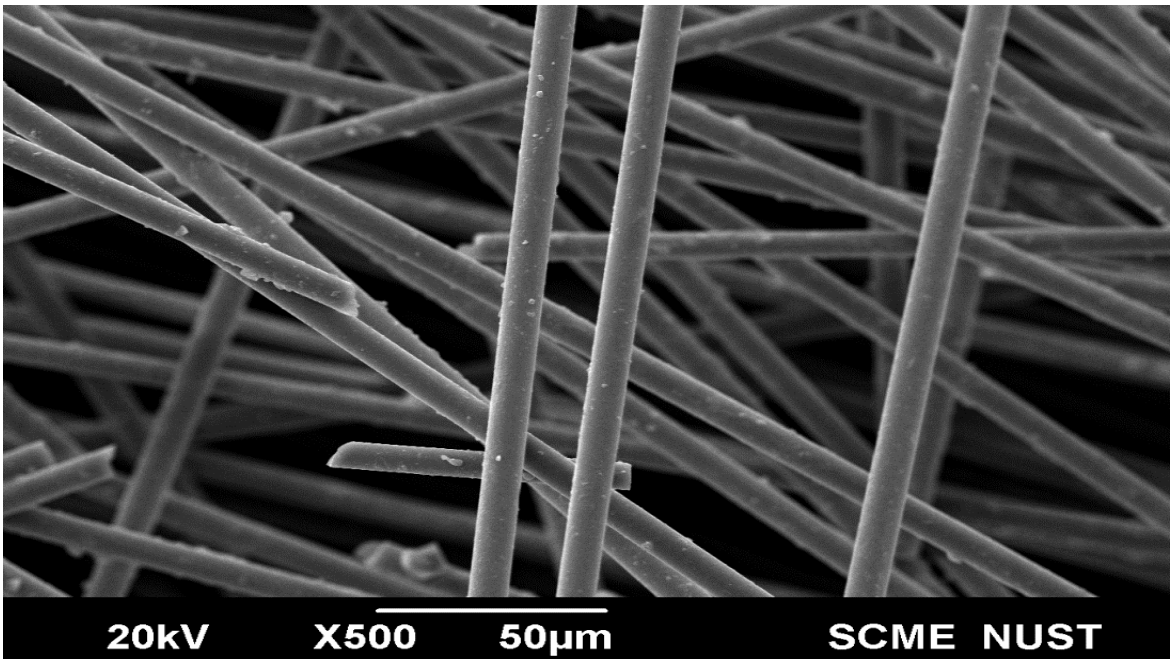

Figure 22: SEM image of sample tile of experiment 2 showing dispersion.

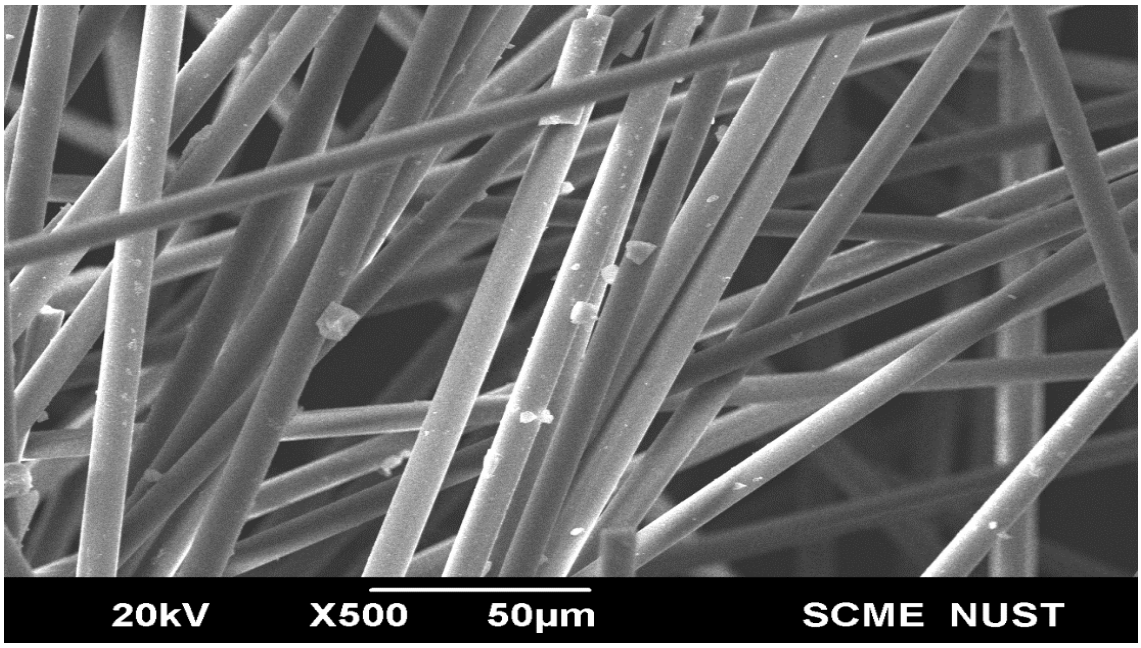

Figure 23: SEM image of sample tile of experiment 2 showing clusters.

4.1.3 Experiment 3

In experiment 3 silica fibers were ultra-sonicated for 5 to 6 hours. This time the sample was not dried on a hot plate as lumps fibers at the end were accumulated at the bottom. So this time vacuum filtration was used for the separation of fibers from the solution. Vacuum filtration squeezed all the solution from the fibers at once and the fibers appeared disoriented.

So again another solution was made where the fibers were ultra-sonicated for 5 to 6 hours. This time for filtration gravity sedimentation method was used where the sample was left overnight to allow water to be drained slowly and rest is evaporated. The dry fibers were then pressed using a hydraulic press to form into circular pellets. One pellet was pressed at 5MPa while the other was pressed at 10MPa. The pellets were then sintered at 1300^{o} C in a muffle furnace with a soaking time of 3 hours.

The SEM images below show the microstructure of the two pellets obtained. Figure 23 is image of tile 1 after sintering pressed at 5MPa before sintering and figure 24 is

the image of tile 2 after sintering pressed at 10MPa before sintering. SEM images show the microstructure of these tiles.

Figure 24: Tile pressed at 10MPA

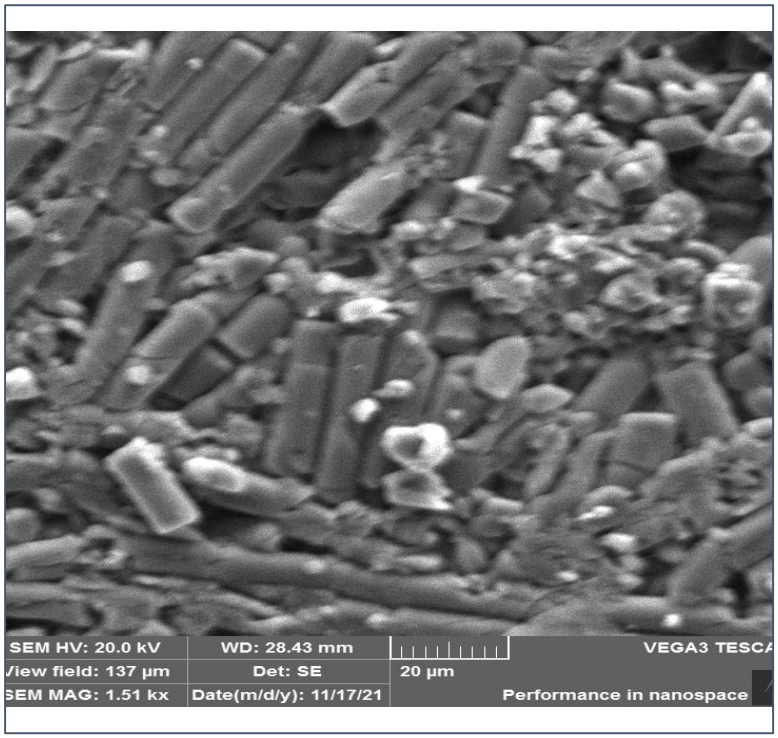

Figure 25: SEM image of tile in fig 23 after pressing and sintering was done

SEM analysis show that the fibers are broken down as their length is reduced as compare to the original specimens. Also some of the fibers are completely damaged as it can be seen in the above image on the right corner. The fibers are shredded into very small pieces. Also no spacing can be seen between the individual fibers that means fibers aren't dispersed properly.

Figure 26: Tile 2 pressed at 5MPa

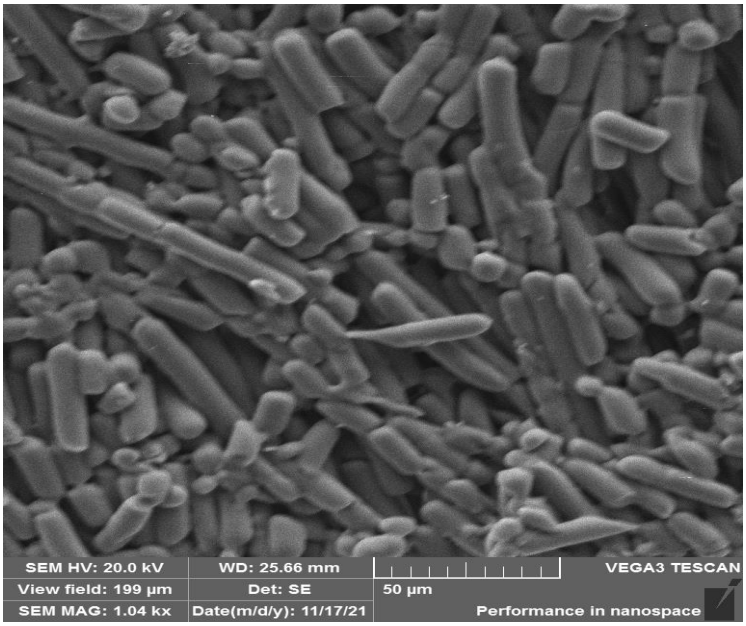

Figure 27: SEM image of tile in fig 26 after pressing and sintering is done.

SEM analysis of pellet 2 also shows fiber broken down and also agglomerated together. The fibers weren't damaged as badly as they were in pellet 1 because of reduced pressure. As a result, conclusion was drawn that high pressure was detrimental to fiber length.

4.1.4 Experiment 4

For this experiment we ultra-sonicated the fibers for 5 to 6 hours. The fibers were filtered by gravity sedimentation method. The single layer of fibers was then mechanically stirred for 2 minutes separate the fibers which were clumped together. The solution was again ultra-sonicated for 5 to 6 hours after which the fibers remain dispersed in the sample and didn't settle at the bottom. The solution was then filtered, dried and sintered at 1300^{o}C.

The SEM image below show the microstructure of this sample tile. Necking at different point shows that sintering has taken place and that the fibers are joined together. The length of the fiber calculated using SEM was 141.28 μm which is greater than the raw silica fibers length indicating that sintering took place. But we can observe some broken fibers as well and their length was calculated to be 37.47μm.

The reasons behind the reduction in the fibers length is longer ultra-sonication time period as it is down twice in the experiment. Another reason of fibers breaking down is mechanically stirring was done for a longer period which damaged the fibers and chopped them off.

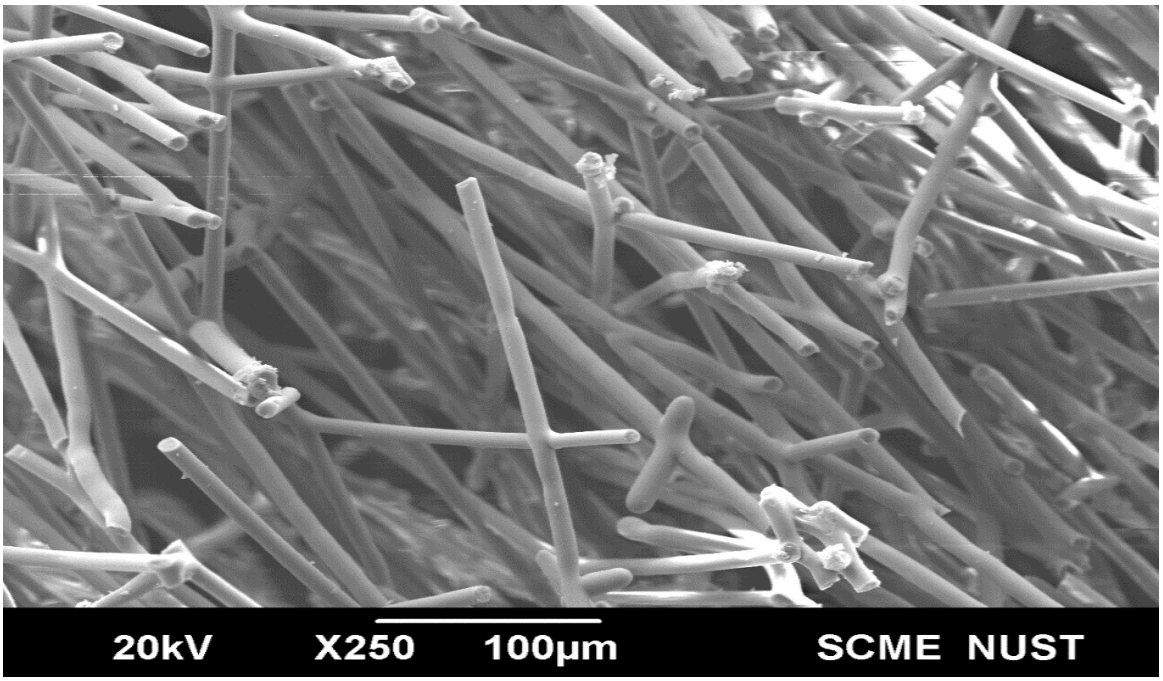

Figure 28: SEM image of tile of experiment 4 after sintering.

4.1.5 Experiment 5

Similar route was followed as in experiment 4 but this time mechanically stirring of the fibers was done for less than a minute. As soon as the single layer produced after first sonication is broken down mechanically stirring was stopped. Also the time for 2nd ultra-sonication was decreased to 4 to 5 hours. The dispersed fibers were then filtered, dried and sintered at 1300°C.

The SEM image shows the microstructure of the sample. Necking can be seen which indicated sintering has taken place. The length of the fibers is 163.18µm which is larger than the raw silica fibers as fibers have joined together. Also no broken fibers can be seen in the sample.

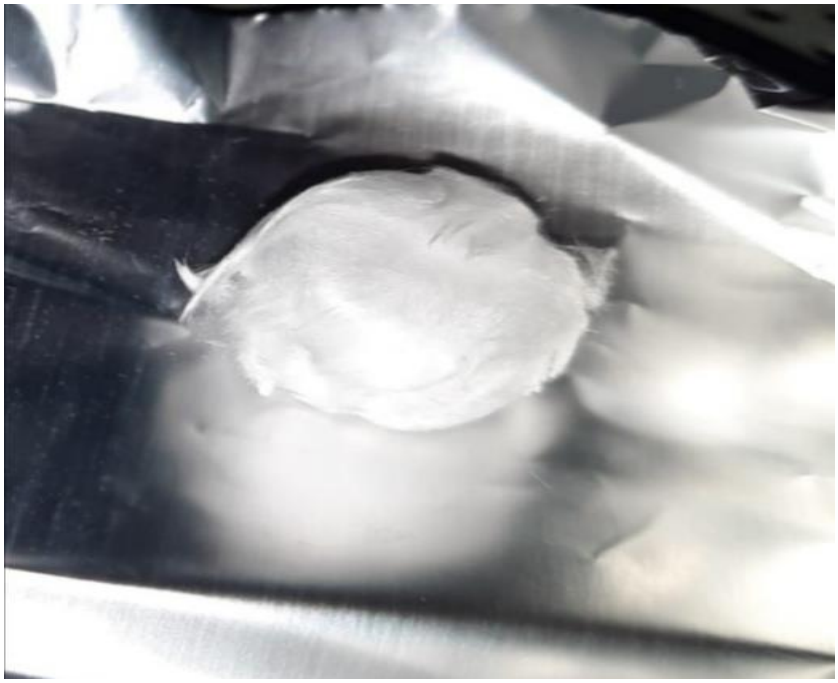

Figure 29: End product of experiment 5

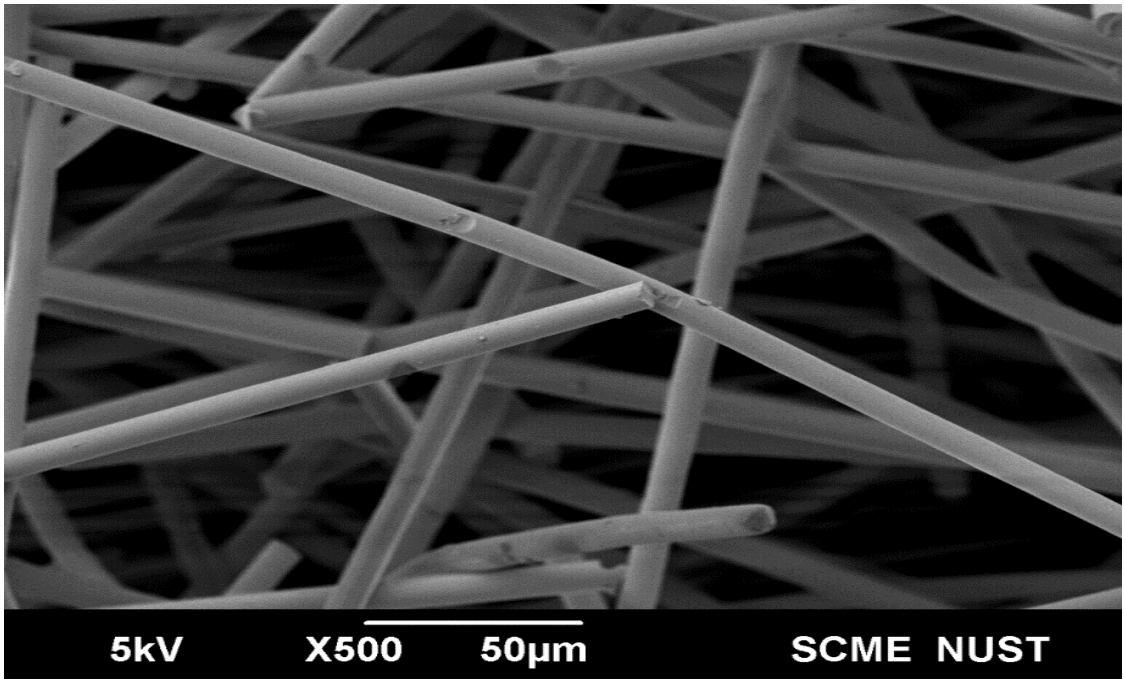

Figure 30: SEM image of tile of experiment 5 after sintering

4.1.6 Experiment 6

In experiment 6 all the procedure was same as in experiment 5 except that in this experiment after filtering and drying, the fibers were sintered at 1350^{o}C. sintering temperature was increased so that better densification can be achieved and the tile can have some improved mechanical properties at such high porosity. The SEM images below shows the microstructure obtained. Visibly spacing between the fibers can be seen.

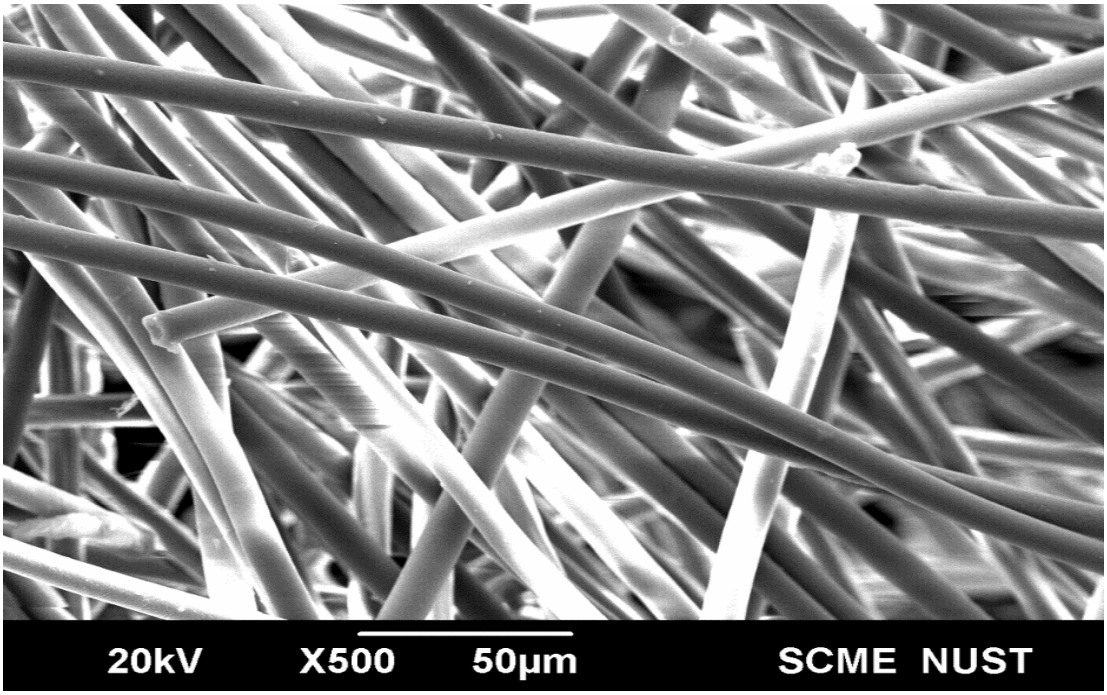

Figure 31: SEM image of sintered tile of experiment 6 showing dispersion

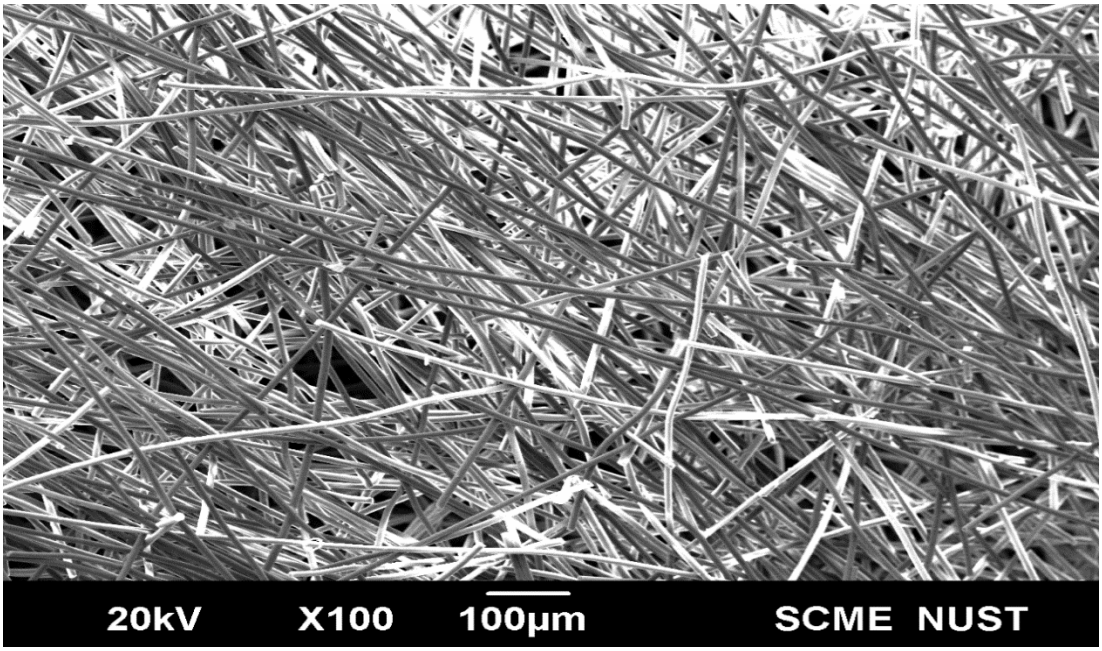

Figure 32: SEM image of sintered tile after experiment 6 showing necking

4.1.7 Conclusion

The deduction about the microstructure of each sample was made by comparing it with that of li-900 so that similar characteristic properties can be achieved. The SEM image below shows the microstructure of li-900 tile which was used as a reference image to draw comparison between our tile and the already present tile system

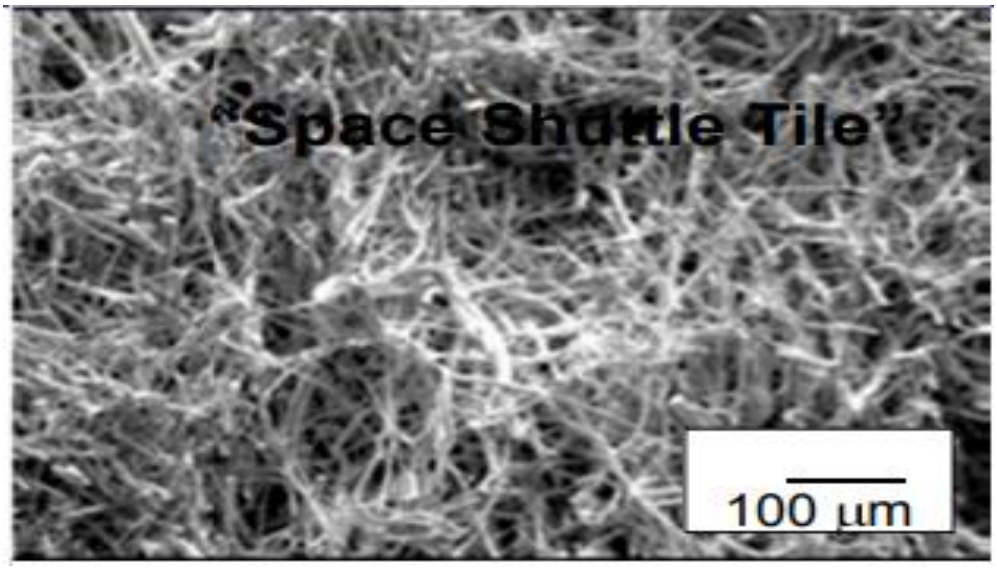

Figure 33: SEM image of li-900 showing the microstructure [8]

So after all these experiments, and comparing the microstructure with that of LI-900 it can be concluded that the best possible route to achieve maximum dispersion in the sample was the one carried out in experiment 6. So all of the next sample tiles were prepared following the procedure carried in experiment 6.

Sample tiles made by this procedure were then pressed at different pressures to vary the consolidation of the fibers before sintering while sintering temperature was kept constant for all of the pressed tiles. These sample tiles porosity was then calculated as they were pressed at different pressures. Testing was then done to measure the thermal conductivity, specific heat and mechanical strength of these tiles and the relationship between percentage porosity and the physical properties was established.

4.2 TESTING

4.2.1 APPARENT POROSITY

Samples were prepared by the variation explained in experiment 6 and then these samples porosity was calculated to confirm the observation that higher dispersion leads to higher porosity levels in the sample. Initially the sample tile's microstructure was observed to make deduction about the dispersion and porosity. Then porosity was calculated to confirm the results deduced after looking at the microstructure of the tile.

The graph below shows the density of the sample as it changes with increasing pressure. A small amount of pressure is required to consolidate the fibers to give them the desired shape and so that their handling can be easy. Varying the pressure applied affected the density of the sample as the height was reduced of our specimen. So it can be concluded that higher the pressure higher is the density of the samples.

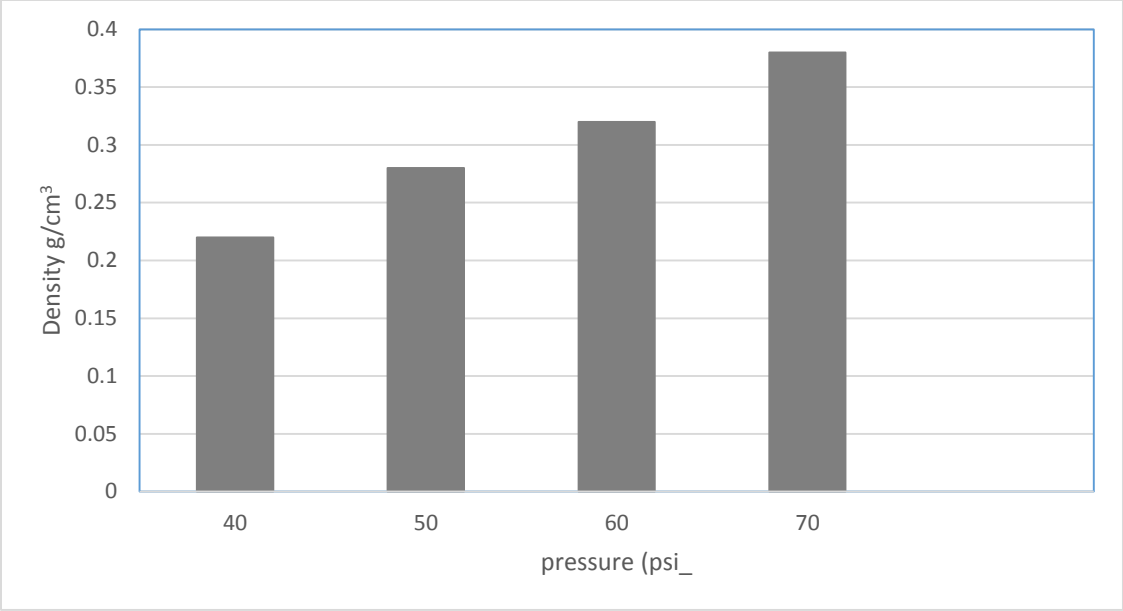

Figure 34: graph showing the relationship between pressure and density.

After this the samples were checked for apparent porosity using the following formula $A = \frac{Ww-Wd}{Ww-Ws}$ x 100%

W_w= weight of wet tile W_d= weight of dry tile

W_s = weight of tile after cleaning surface.

The graph below shows the value of apparent density calculated of the above samples. It can be observed that higher the density lower is the percentage porosity in the sample. The reason behind in this as pressure is increased to enhance the densification the fibers move in the empty spaces in the sample as a result of which the porosity of the samples is reduced.

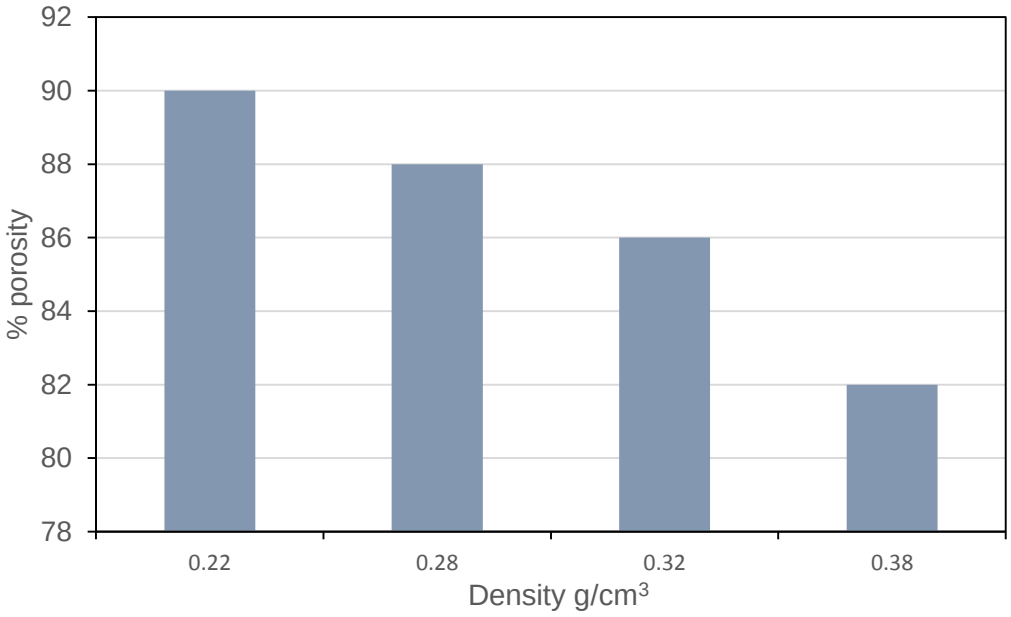

Figure 35: graph showing relationship between density and %age porosity

4.2.2 BET (Brunauer-Emmett-Teller) surface analysis

These samples porosity was then checked by BET. BET gave data about the surface area and pore volume of each sample. The graph below shows the result of BET analysis. It can be seen in the graph that the sample surface area is directly proportional to perchance porosity. More porosity present great is the surface area of the sample.

Total pore volume is also related to the surface area. Larger the surface area more pores present hence larger the total pore volume which can also be observed in the graph below.

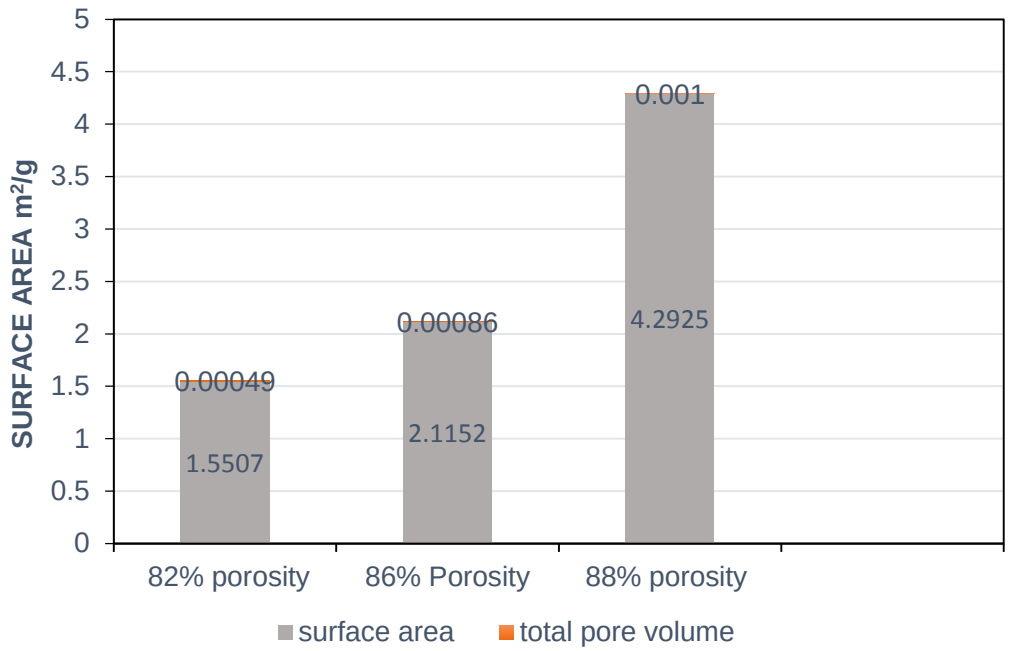

Figure 36: graph showing relationship between %age porosity and surface area.

4.2.3 Thermal conductivity testing

High percentage of porosity in the samples was required so that thermal conductivity was reduced and the tile do not heat up during re–entry. The samples were then tested to calculate their thermal conductivity. Each of the sample was heated at 25°C, 100°C, 200°C and 300°C. The graph below shows the result of the test.

It can be observed that as the porosity is increased the overall value of thermal conductivity is decreases. In each sample the small increase in thermal conductivity is due to the increase in temperature. Initially as temperature is increased lattice vibrations and the movement of the atoms result there is some increase in the thermal conductivity of the samples. So the results show that with increased porosity thermal conductivity decreases one of the main objective of our project.

Also the graph shows thermal conductivity values of li-900 given in literature at the same temperatures [24]. Comparing the results, we can see that the value of li- 900 value is almost equal to that of the sample with 88% porosity level. Li-900 tiles are

made with 90% porosity which accounts for even lower thermal conductivity values of li-900 at similar temperatures.

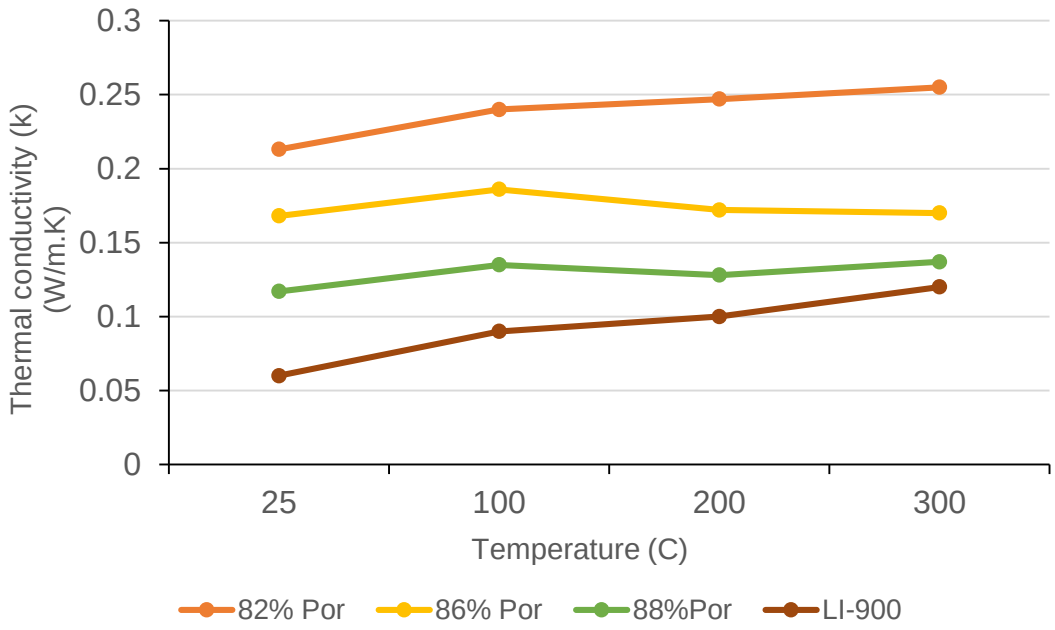

Figure 37: graph showing relationship between %age porosity and thermal conductivity.

The graph below shows the value of specific heat (the heat required to raise the temperature by 1 kelvin) absorbed by the samples changing with the amount of percentage porosity present. Further the results are compared with li-900 tiles specific heat value obtained from literature [25].

It can be observed that as the sample porosity increases the amount of energy required to raise the temperature decreases. The value of li-900's specific capacity is the smallest since it has 90% porosity. This decrease in specific capacity is because as porosity is increased less fibers for thermal conduction hence these fibers can heat up with less energy. But the porosity present creates hindrance in the flow of thermal energy hence thermal conductivity of the fibers is reduced at lower values of specific heat.

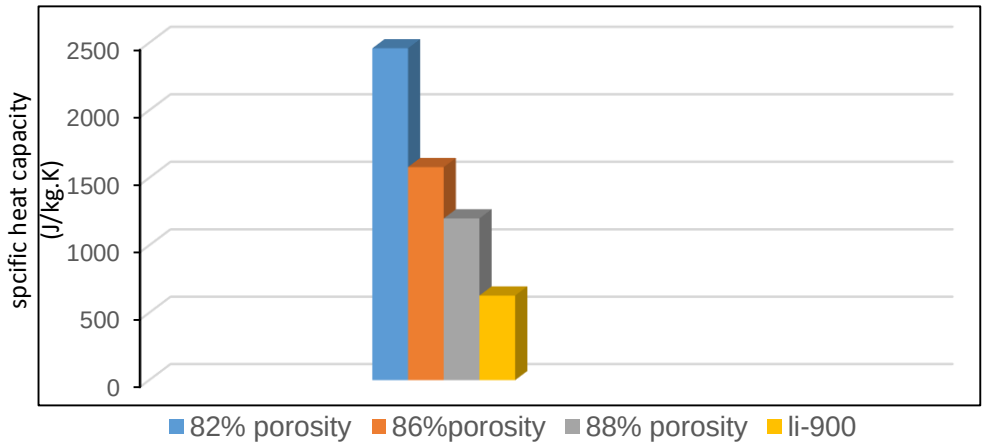

Figure 38: Graph showing relationship between %age porosity and specific heat.

4.2.4 Compression Testing

Compression testing of the samples was done to determine the strength of these tiles and the maximum pressure they can withstand. The test was performed with a strain rate of 0.1mm/min and 1mm/min. No compression strength value was obtained for samples with porosity 88% and 86% as the fibers didn't remain intact because of the high porosity hence the results were inconclusive. Compression strength value for 82% sample was obtained in the range 0.58-0.60MPA.

From literature we can deduce the compression strength value of li-900 to be around 0.42 – 0.48MPa. [25] The value of compression strength for li-900 is low because o the reason that li-900 tiles are made with up to 90% porosity. Due to this porosity, fiber can dislodge when pressure is applied hence gives lower value of compression strength as compare to our sample with 82% porosity that have higher value for compression strength.

CONCLUSION

Thermal protection system (TPS) has become immensely important with the passage of time. As missiles and space crafts are being send into space to gather information about other planets and the solar system. One need these space crafts and missiles to return back without any damage to outer body so that they can reused as it takes a lot of resources, revenue and time to produce a single aircraft. This is where TPS come into action as it provides an outer covering of insulation for the space craft's body preventing it from extreme weather conditions.

TPS systems are being studied everywhere and work is being done. Similarly, in Pakistan work is being done to produce this kind of insulation system that can protect our missile and aircrafts as already they are few in numbers. One of the most prevalent insulation tile being used to provide thermal insulation is li-900 mainly used by NASA in all of its space crafts. Efforts are being made to create an insulation tile with similar characteristics that can provide insulation.

In our project the tile made out of quartz silica fibers showed promising results when comparison was made between our sample tile and that of li-900 results. First of all, a number of variations in the procedure were carried out in order to ensure the maximum dispersion of the silica fibers. This was the most difficult step as the fibers were agglomerated very easily. Once the route by which fibers dispersion was maximum circular tile was made after sintering. The tiles were then sent for testing to check for porosity and thermal conductivity. The main aim of the project was to manufacture tiles that have high porosity, low thermal conductivity and moderate strength. A compromise was made with the tiles strength as thermal conductivity was our main objective that was induced because of high porosity.

The best sample tile out of all was the one with 88% porosity level as its results were closest to that of li-900. Initially analysis about dispersion in the samples were made by observing the microstructure using SEM images. The effect of pressure on density and porosity was studied that showed at lower pressure density decreases but

porosity increases. This porosity was then measured by calculating the apparent density and from BET by analyzing the surface area. The increase in porosity then led to lower values of thermal conductivity. The values of specific heat also showed a trend as the porosity was increased the value of specific heat reduced. Last characterization technique was compression testing which gave inconclusive results for 88% sample as at this porosity the fibers didn't remain intact. But we were able to achieve the main objectives of our project which were to produce tiles that have higher porosity levels and reduce thermal conductivity at higher temperatures.

The future prospects of this project can be the use of some other fibers such as alumina or Nextel along with silica fibers that can provide enhanced structural integrity to our sample tile along with reduced thermal conductivity. Also different coatings can be applied like RCG (reaction cured glass) or TUFI (toughened unipiece fibrous insulation) to the tile surface to enhance the surface durability and emissivity of heat from the surface during high temperature conditions.

REFERENCES

1. Johnson, Sylvia M.; Squire, Thomas H.; Lawson, John W.; Gusman, Michael; Lau, K-H; Sanjuro, Angel (January 30, 2014). *Biologically-Derived Photonic Materials for Thermal Protection Systems* [1]
2. . Anderson, John D. Jr. (January 2001) (1984), *Fundamentals of Aerodynamics* (3rd ed.) [2]
3. *A Space Shuttle Chronology*, by John F. Guilmartin and John Mauer (NASA Johnson Space Center, 1988) [3]
4. Marcia Dunn (February 2, 2003). "*Columbia's problems began on left wing*". [4]
5. Gore, Rick (March 1981). "When the Space Shuttle Finally Flies" [5]
6. Jenkins, Dennis R. (2007). *Space Shuttle: The History of the National Space Transportation System*. [6]
7. *Thermosets; structure, properties and applications* (2nd edition). Edited by Qipeng Guo. [7]
8. *Thermal Protection Materials: Development, Characterization and Evaluation.* Sylvia M. Johnson Entry Systems and Technology Division NASA Ames Research Center. [8]
9. José Meseguer, Isabel Pérez-Grande and Angel Sanz-Andrés (2012). "*Space Craft Thermal Control".* [9]
10. Deepak Nelmangala Chandrashekhar , Guntumadugu Girish Raj , Akshay Gowda Nanjunda. "Properties *and Appliaction of Ablative Materials".* [10]
11. Orbiter Thermal Protection System. *Alvaro Rodriguez, Cooper Snapp.* [11]
12. *"SPACE SHUTTLE TILES",* Mohammed Jiruwala. [12]
13. https://en.m.wikipedia.org/wiki/Space_Shuttle_thermal_protection_system [13]
14. Vann Heng, Buena Park, CA (US); Karrie Ann Hinkle, Aliso Viejo, CA (US); Mary Ann Santos, West Covina, CA (US)/ US 2004.0033881A1. [14]
15. https://www.toppr.com/ask/en-au/content/concept/gay-lussacs-law-of-combining-volumes-202778/ [15]

16. https://physics.stackexchange.com/questions/535582/why-can-atmospheric-re-entry-heat-up-the-air-into-plasma [16]
17. https://www.quora.com/Why-isnt-the-NASA-thermal-protection-system-used-for-firefighters [17]
18. https://www.sciencedirect.com/topics/materials-science/ablative-material [18]
19. https://www.nasa.gov/centers/glenn/shuttlestation/shuttle/G_RTF_image_feature_9.html [19]
20. https://www.quora.com/The-space-shuttle-heat-shield-tiles-LI-900-were-made-of-silica-fibers-obtained-from-sand-Can-you-tell-me-if-it-was-quartz-The-answers-on-the-web-are-a-bit-contradictory [20]
21. https://www.nasa.gov/centers/ames/thermal-protection-materials/tps-materials-development/reusable.html [21]
22. https://govinfo.library.unt.edu/caib/photos/view37ea.html-photo_id=507.htm [22]
23. Monique Strider, Eric Keven Silva, M Angela, A. Mierles. Specific energy; a new approach to Ultrasound assisted extraction of natural colorants. (2019/9/2) [23]
24. Thermomechanical Analysis of a thermal protection system with defects. Collection of Technical Papers - AIAA/ASME/ASCE/AHS/ASC Structures, Structural Dynamics and Materials Conference [24]
25. http://mae-nas.eng.usu.edu/MAE_5420_Web/section3/appendix3.pdf [25]
26. D.J geen, Non destructive evaluation of low density fibrous ceramics. [26]